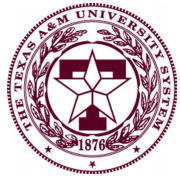


The 12th RHIC BES theory and experiment online seminar

Probing QCD Critical Point with Light Nuclei Production *in Heavy-Ion Collisions*



TEXAS A&M
UNIVERSITY®

KaiJia Sun (孙开佳)

kjsun@tamu.edu

Cyclotron Institute

10/20/2020

In collaboration with Che-Ming Ko, Lie-Wen Chen, Zhangbu Xu, Feng Li, Jun Xu, Jie Pu, Benjamin Dönigus, Xiaofeng Luo, Jinhui Chen, and Tianhao Shao

Outline

1. Background and motivation
2. Production mechanisms of light nuclei in high-energy nucleus collisions
3. QCD criticality on light nuclei production
4. Effects of the first-order chiral phase transition on light nuclei production within a transport approach
5. Summary

Reference:

K. J. Sun, C. M. Ko, and F. Li, arXiv:2008.02325(2020)

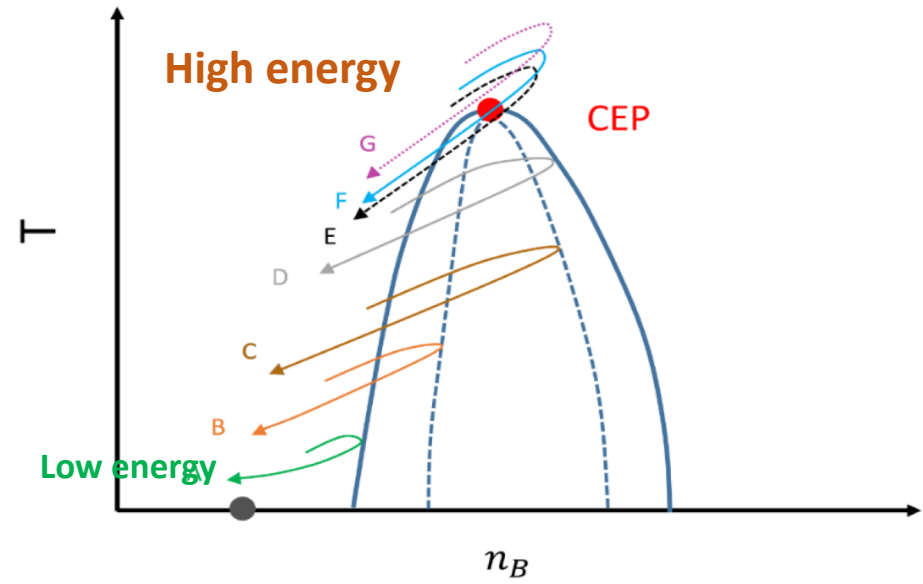
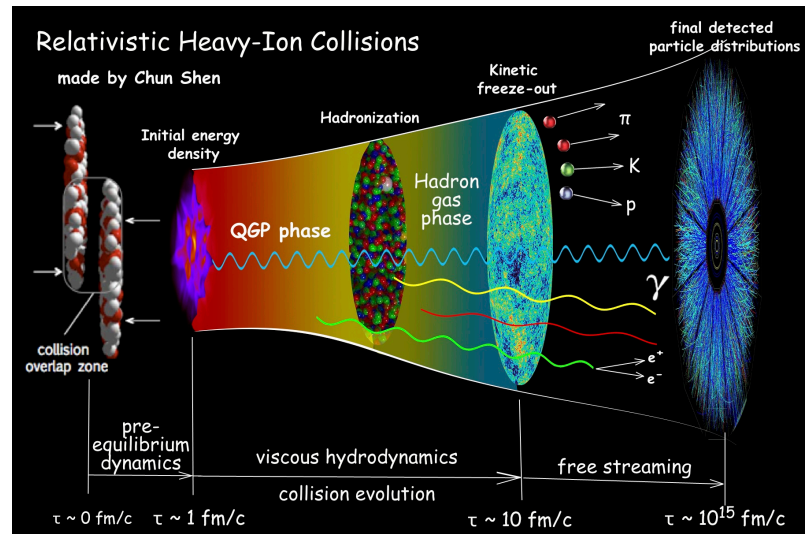
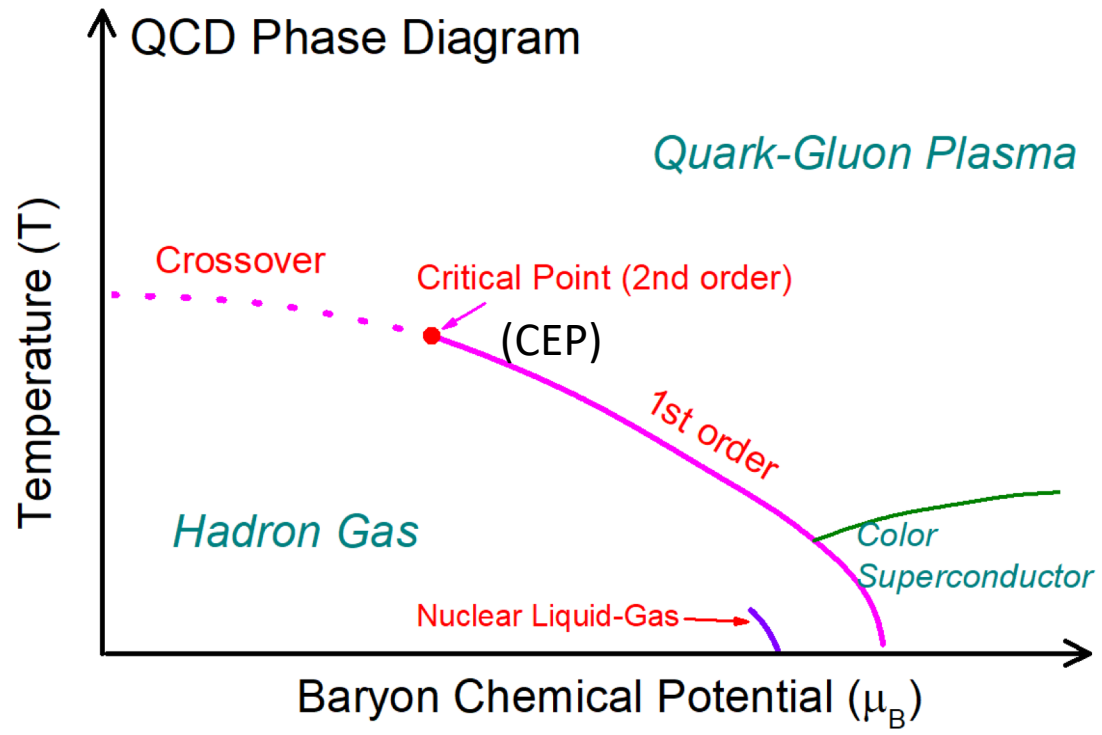
K. J. Sun, C. M. Ko, F. Li, J. Xu, and L. W. Chen., arXiv: 2006.08929(2020)

K. J. Sun, L. W. Chen, C. M. Ko, and Z. Xu., Phys. Lett. B 774, 103 (2017)

K. J. Sun, L. W. Chen, C. M. Ko, J. Pu, and Z. Xu., Phys. Lett. B 781, 499 (2018)

K. J. Sun, C. M. Ko, and B. Dönigus Phys. Lett. B 792, 132 (2019)

1. QCD phase diagram

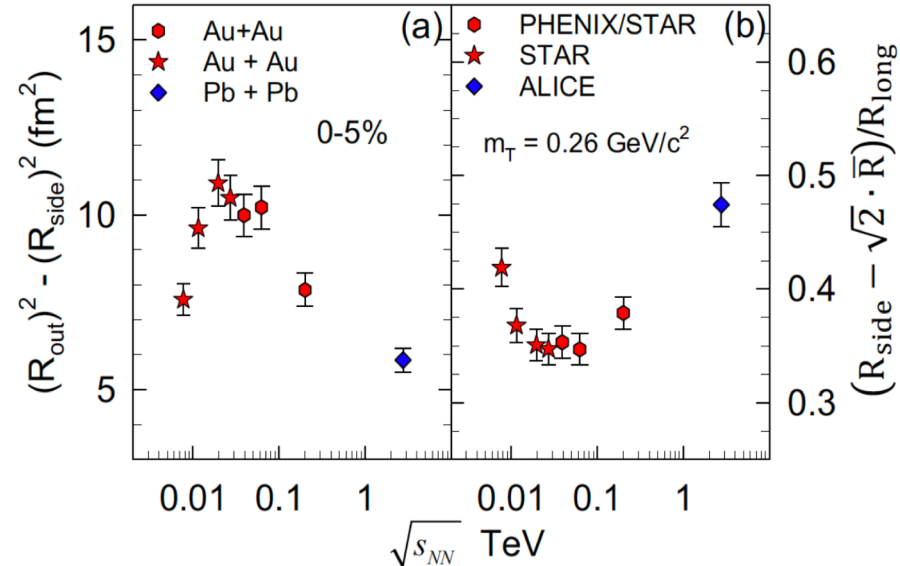
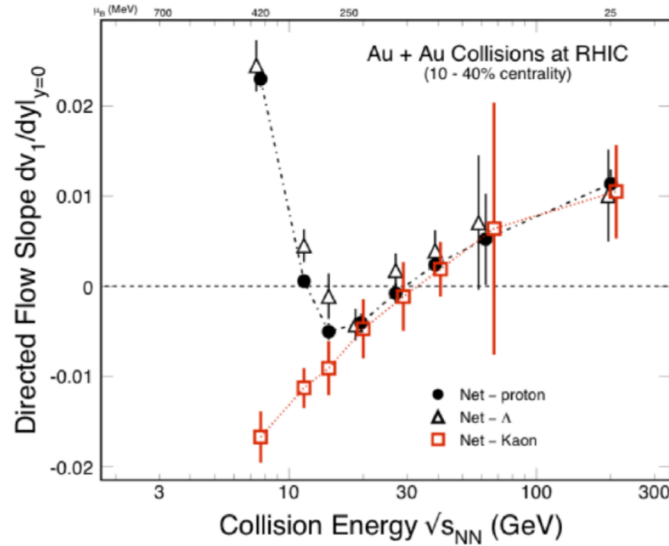


X. Luo and N. Xu, Nucl. Sci. Tech. 28, 112 (2017)
A. Bzdak et al., Phys. Rept. 853, 1 (2020)

Non-monotonic behavior is expected!

1. Non-monotonic behavior

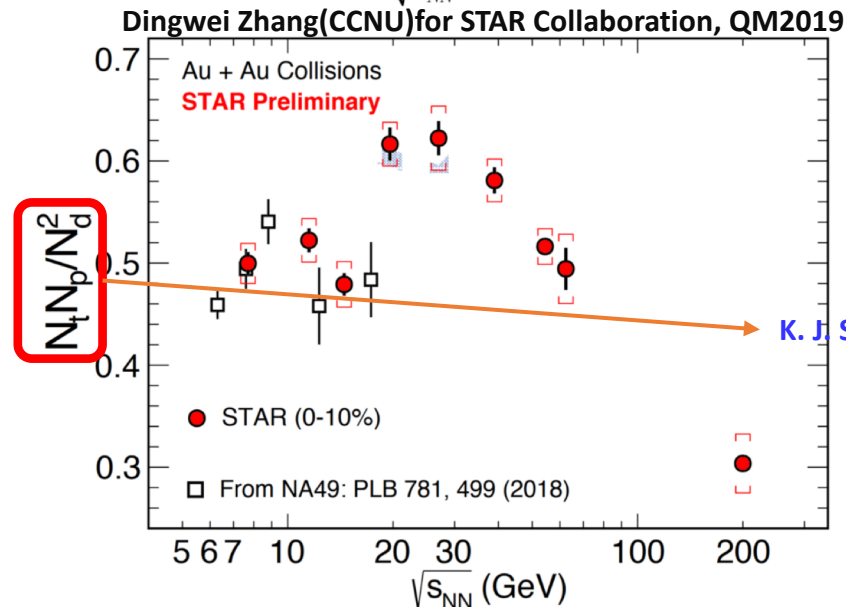
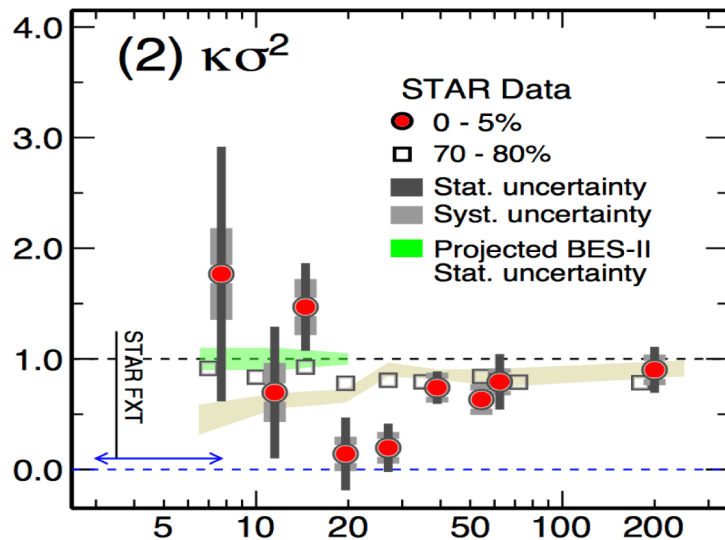
(2)



All the non-monotonic behaviors are expected to be related to either the first-order or second-order phase transition from QGP to hadronic matter.

Q1. Why the signals are all at around 20 GeV?

Q2. Any connections between these signals?



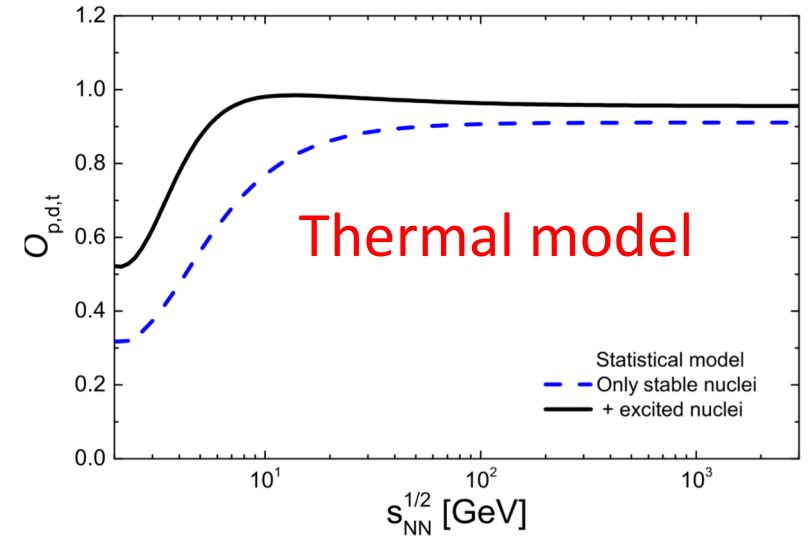
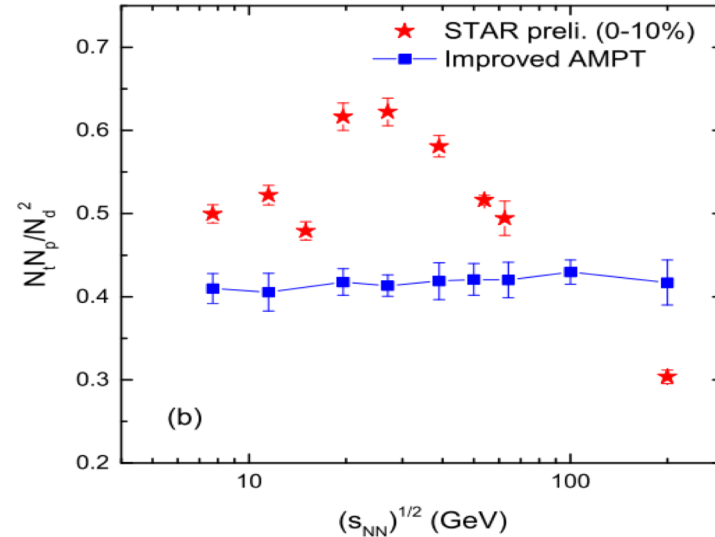
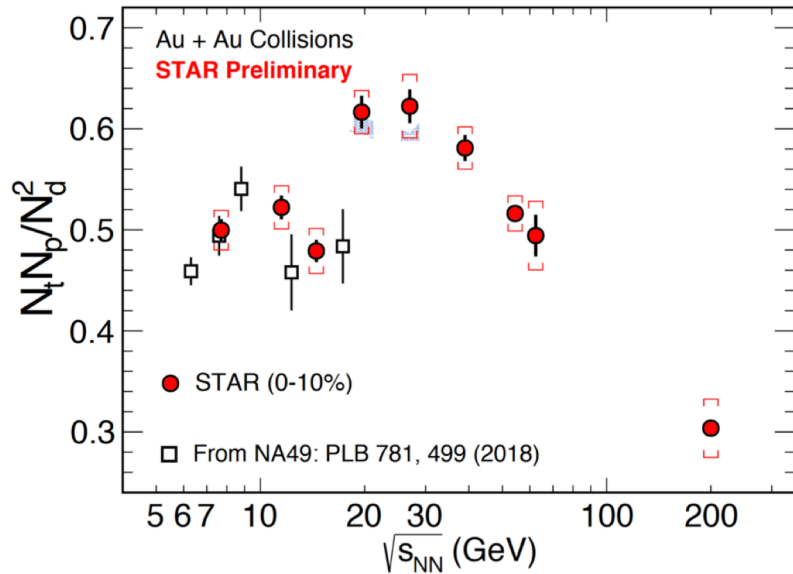
K. J. Sun, L. W. Chen, C. M. Ko, and Z. Xu., Phys. Lett. B 774, 103 (2017)

A. Bzdak et al., Phys. Rept. 853, 1 (2020)
 STAR: arXiv:2001.02852(2020); PRL 112, 162301 (2014); PRL 120, 062301(2018);
 R. A. Lacey, PRL 114, 142301 (2015);

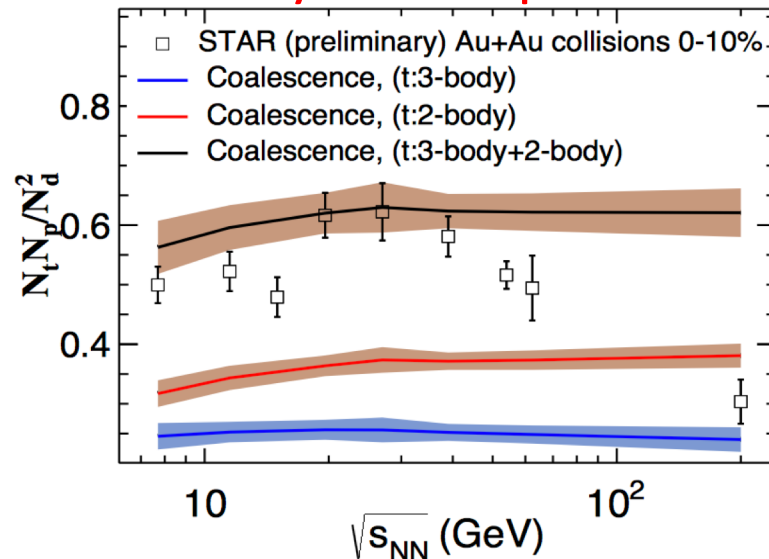
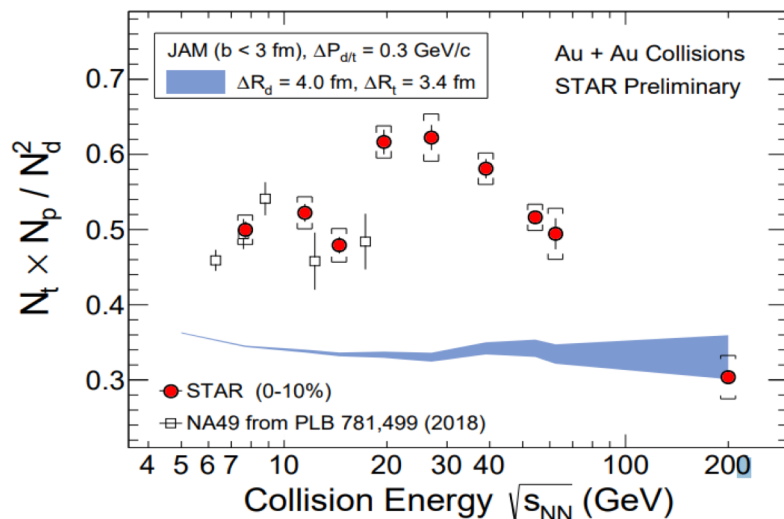
1. Non-monotonic behavior of tp/d^2

(3)

Dingwei Zhang(CCNU)for STAR Collaboration, QM2019



Hydro+Urqmd

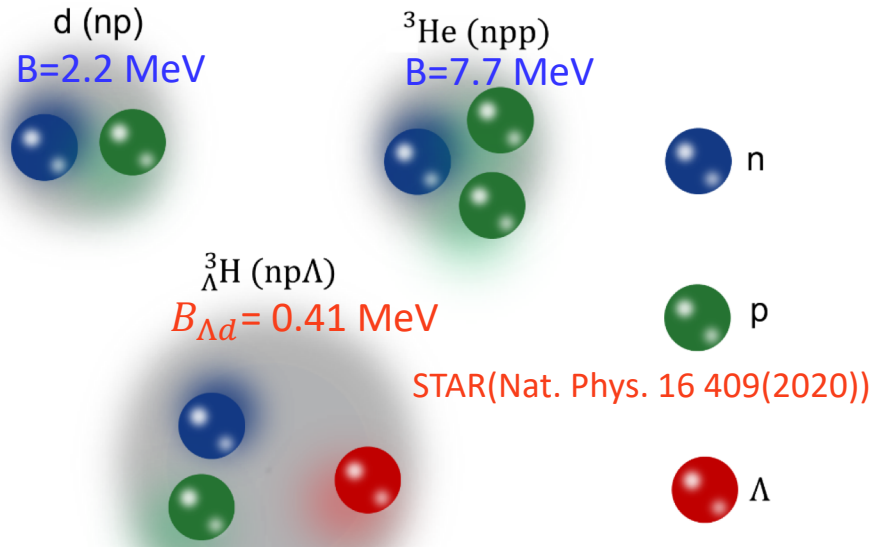


No model can explain the data!

W. Zhao et al., arXiv:2009.06959(2020)
 D. Zhang (STAR), arXiv:2002.10677(2020)
 H. Liu et al., Phys. Lett. B805, 135452 (2020)
 V.Vovchenko et al., arXiv:2004.04411(2020)
 K. J. Sun and C. M. Ko, arXiv:2005.00182(2020)

2. Light nuclei production mechanisms in high-energy nucleus collisions

2. Production mechanisms of light cluster in high-energy nucleus collisions (4)



Deuteron (np)

Triton (nnp)

Helium-3 (npp)

Hypertriton (np Λ)

Helium-4 (nnpp)

\bar{n}

\bar{p}

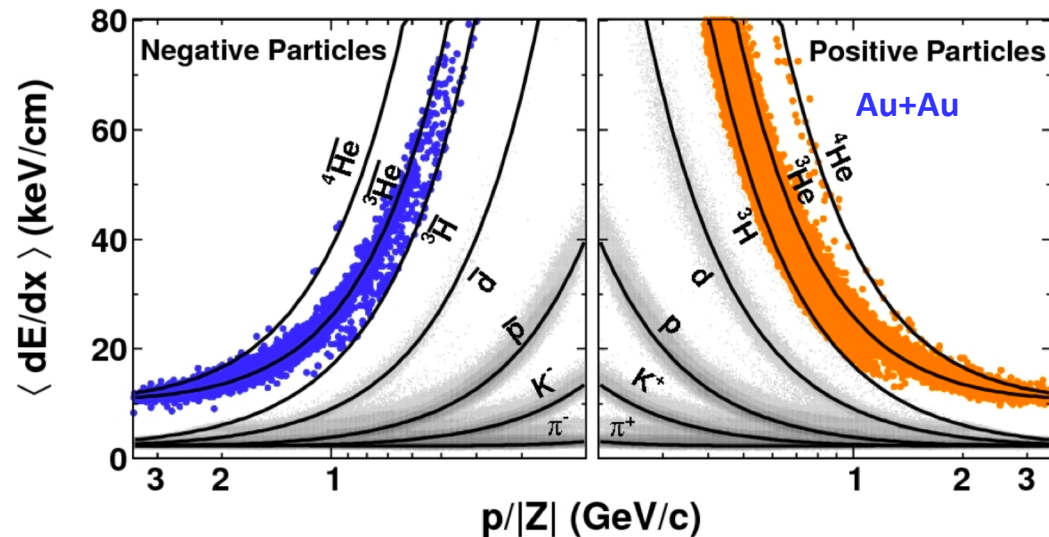
$\bar{\Lambda}$

\bar{d}

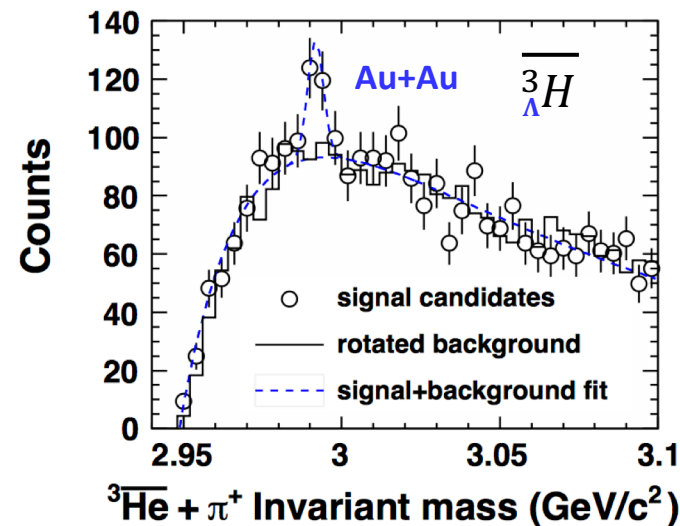
${}^3\bar{\text{He}}$

${}^3_{\Lambda}\bar{\text{H}}$

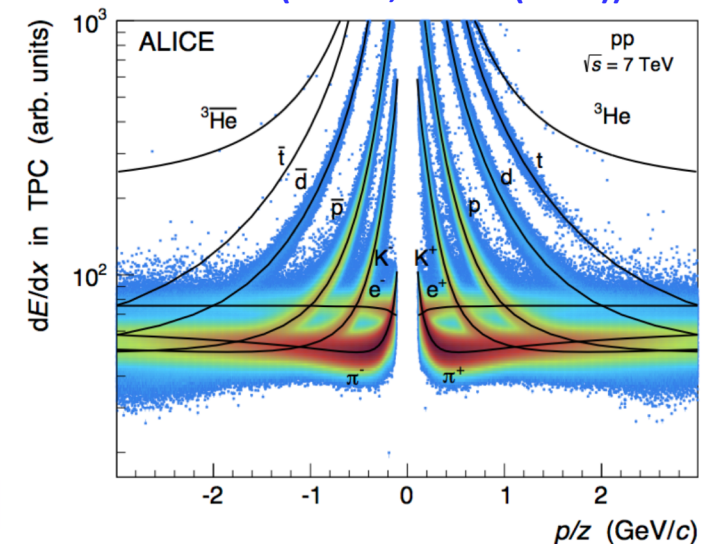
STAR (Nature 473.353(2011))



STAR (Science 328, 58(2010))



ALICE (PRC93,024917(2015))



2. Production mechanisms of light cluster in high energy nucleus collisions (5)

⊗ Thermal emission $N_A \approx g_A V (2\pi m_A T)^{3/2} e^{(A\mu_B - m_A)/T}$

A. Andronic, P. Braun-Munzinger, J. Stachel, H. Stöcker, PLB 697, 203 (2011)

A. Andronic, P. Braun-Munzinger, K. Redlich, J. Stachel, Nature 561, 321 (2018)

V. Vovchenko et al., PLB800, 135131 (2020)

⊗ Coalescence (density matrix formalism) $N_A = \text{Tr}(\hat{\rho}_s \hat{\rho}_A) = g_c \int d\Gamma \rho_s(\{x_i, p_i\}) \times W_A(\{x_i, p_i\})$

H. Sato and K. Yazaki, PLB98, 153 (1981); E. Remler, Ann. Phys. 136, 293 (1981); M. Gyulassy, K. Frankel, and E. Remler, NPA402,596 (1983);

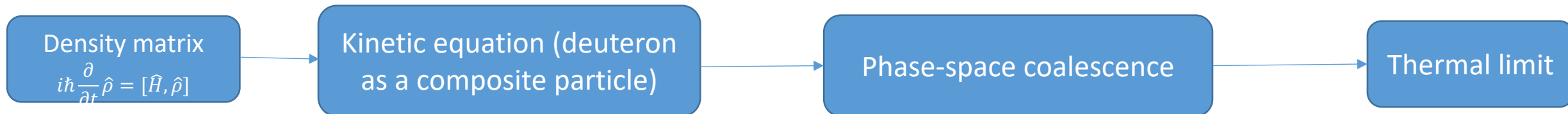
S. Mrowczynski, J. Phys. G 13, 1089 (1987); S. Leupold and U. Heinz, PRC50, 1110 (1994); R. Scheibl and U. W. Heinz, PRC59, 1585(1999);

⊗ Kinetic equation $\pi NN \leftrightarrow \pi d, NNN \leftrightarrow Nd, NN \leftrightarrow \pi d,$
 $\pi NNN \leftrightarrow \pi t, NNNN \leftrightarrow Nt, NNN \leftrightarrow \pi t, \pi Nd \leftrightarrow \pi t, NNd \leftrightarrow Nt, Nd \leftrightarrow \pi t$

A.Z. Mekjian, PRC17,1051 (1978); P. Danielewicz, G.F. Bertsch, NPA533, 712 (1991); P. Danielewicz and P. Schuck, PLB274, 268 (1992);

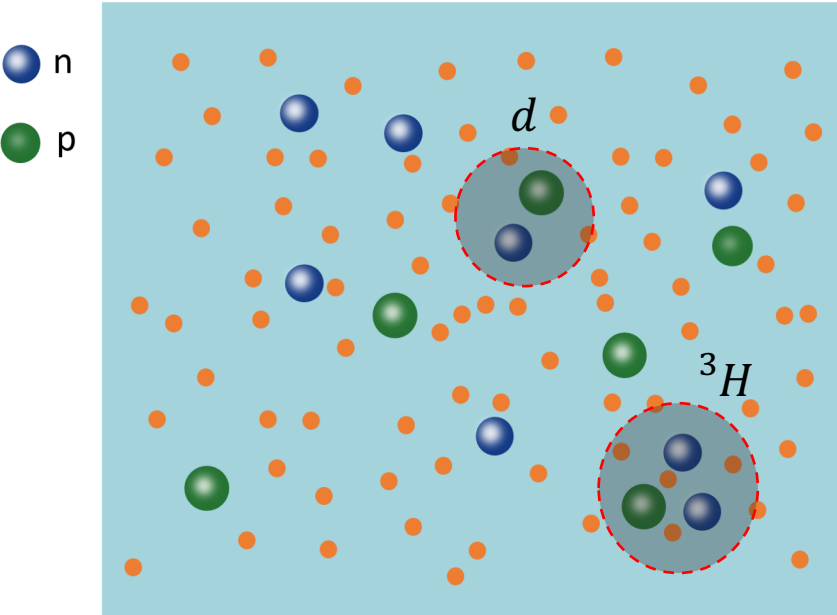
Y. Oh and C. M. Ko PRC76, 054910(2007); PRC80, 064902(2009); D. Oliinychenko, L. G. Pang, H. Elfner, and V. Koch, PRC99, 044907 (2019);

Relationship between these mechanisms



2. Phase-space coalescence model

(6)



$$N_d = \frac{3}{4} \int d\Gamma f_{pn}^w(\vec{p}_1, \vec{r}_1, \vec{p}_2, \vec{r}_2) \times W_d(\vec{r}, \vec{p}) \quad W_d(\vec{r}, \vec{p}) = \frac{1}{\pi\hbar} \int d\vec{r}' \psi_d^*(\vec{r} + \vec{r}') \psi_d(\vec{r} - \vec{r}') e^{2i\vec{p}\cdot\vec{r}'}$$

Key observations:

1. The deuteron production encodes the phase-space information of nucleons, in particular, the density fluctuation and correlation.
2. For small emission source, the deuteron's wavefunction affects (suppresses) its production probability. A true quantum effect predicted long time ago. (see e.g. R. Scheibl and U. W. Heinz, PRC59. 1585(1999);)

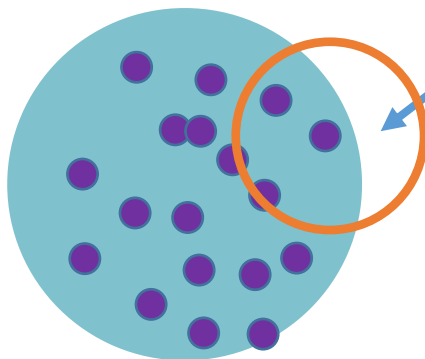
Note the HBT correlation of a pair of neutron and proton is proportional to

$$\int d\Gamma f_{pn}^w(\vec{p}_1, \vec{r}_1, \vec{p}_2, \vec{r}_2) \times W_{np}^{pair}(\vec{r}, \vec{p})$$

3. The deuteron production is closely related to the HBT correlation of nucleons. Similar source information can be extracted from both HBT and deuteron production as first pointed out by Mrówczyński(PLB248, 459 (1990))

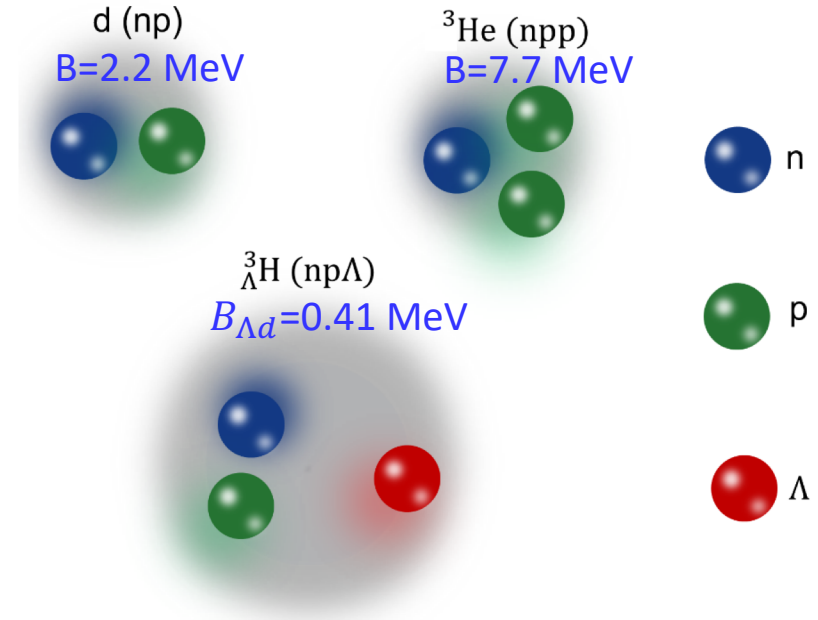
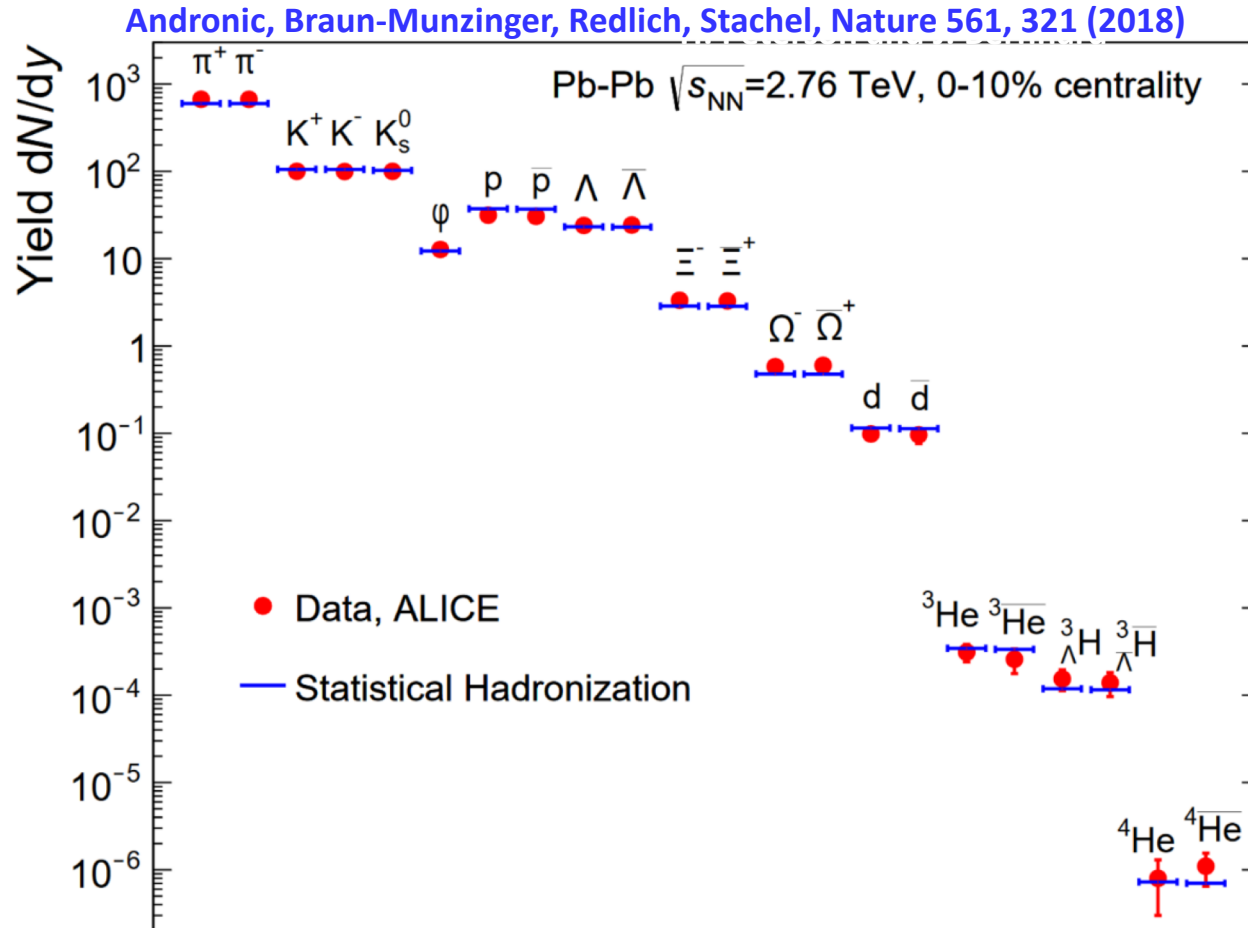
Above are also true for heavier nuclei.

Light Nuclei provide an unique tool to study the density fluctuation and correlation



2. Light cluster production in AA collisions

(7)



1. Rarely produced, suppression by $e^{-m_A/T}$
2. Binding energies (E_B) \ll hadronization temperature (~ 155 MeV)
The size $r \sim \frac{1}{\sqrt{4\mu E_B}}$, ($r_d \sim 2$ fm, $r_{{}^3\text{He}} \sim 2$ fm, $r_{{}^3\text{H}} \sim 5$ fm)

'snow ball in hell'

Thermal model assumes that the hadronic interactions do not affect the yield of light cluster from hadronization to kinetic freezeout. For deuteron, this has been confirmed by D. Oliinychenko et al. (PRC99, 044907 (2019)). The main reason is the **large cross sections** of $d+h \leftrightarrow NN+h$ (See Dima's talk for details)

2. Light cluster production in AA collisions

(8)

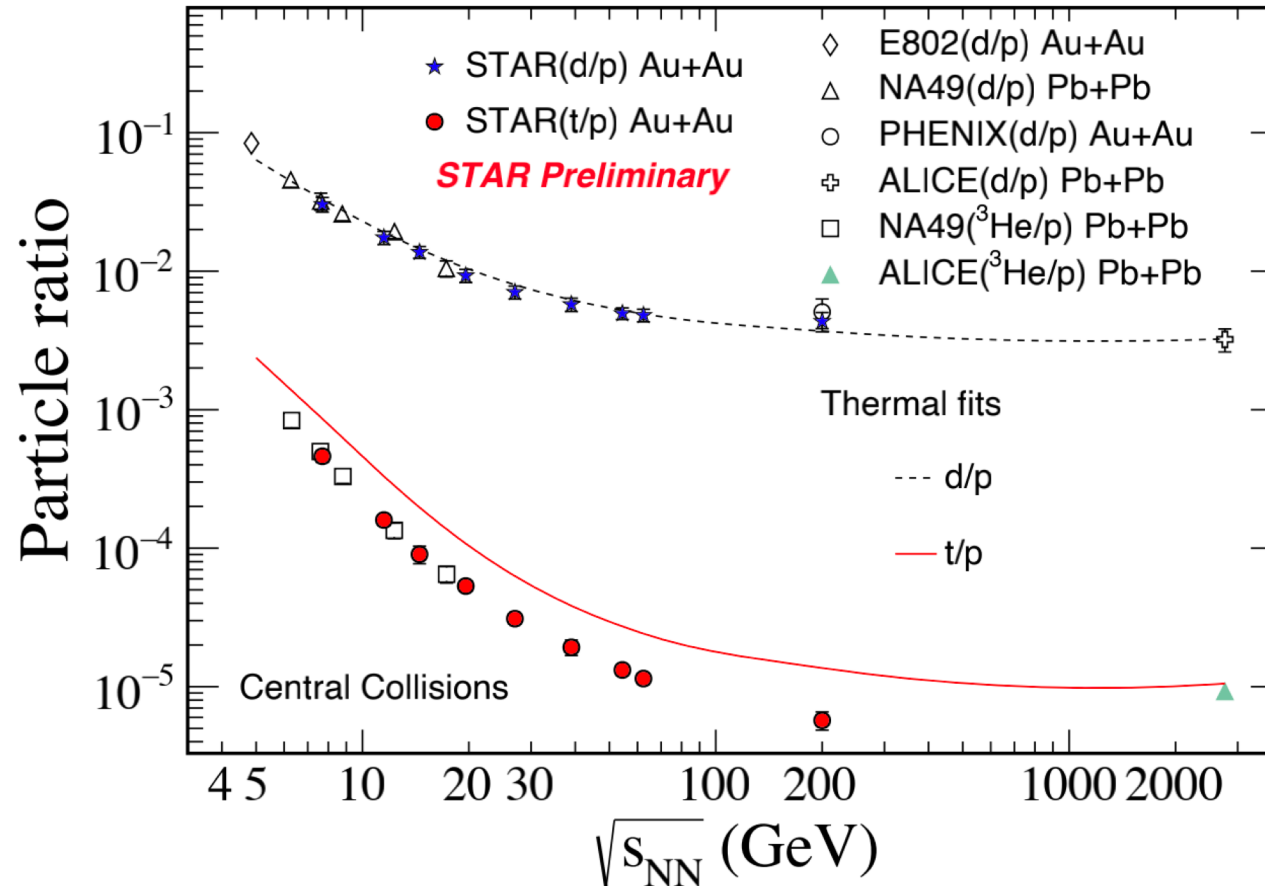


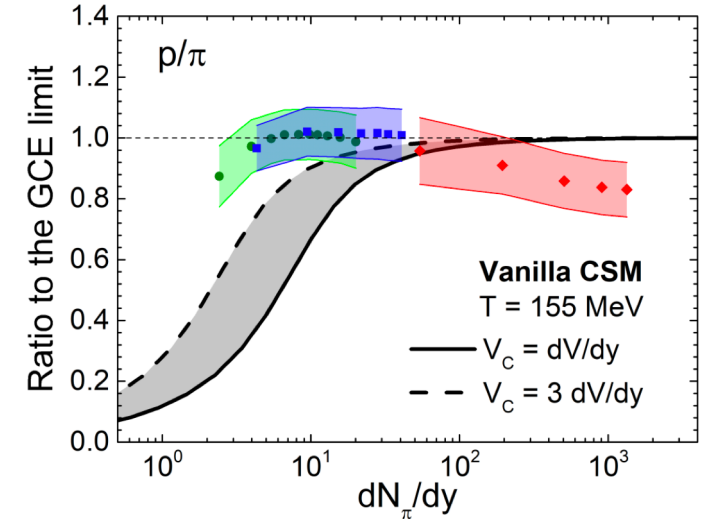
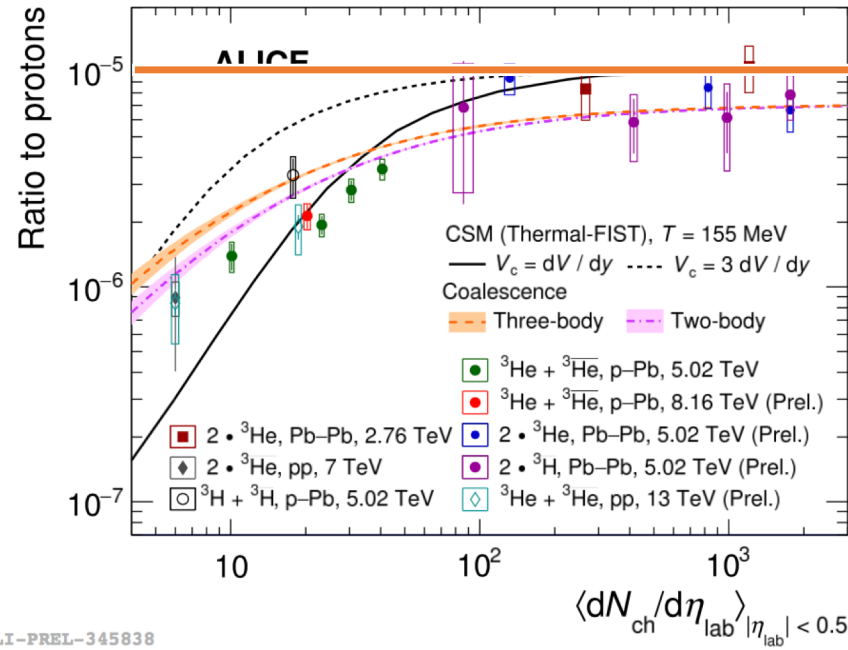
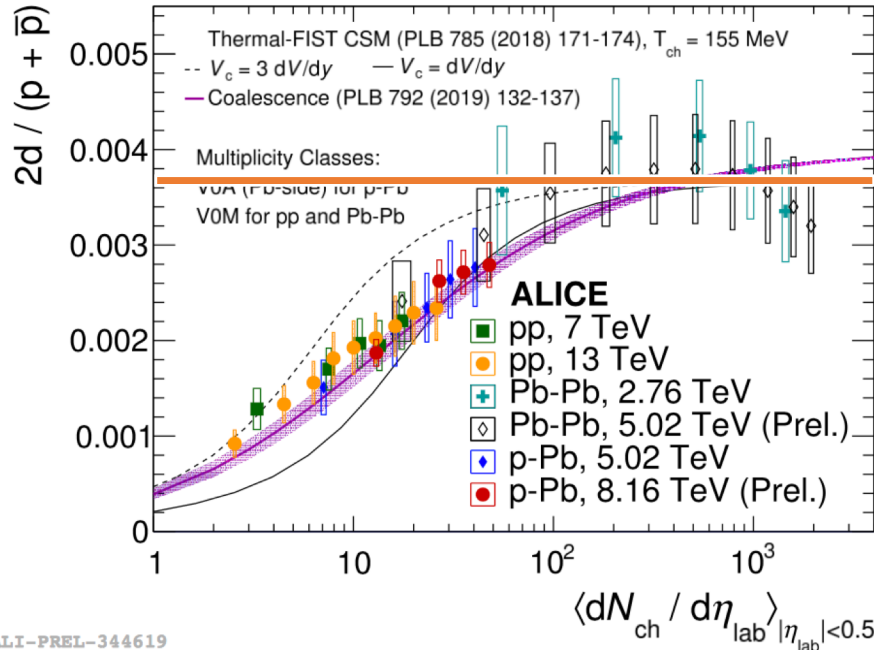
Figure from XiaoFeng's talk

1. The d/p ratio can be well described by thermal model
2. t/p ratio are significantly below the thermal model predictions at RHIC and SPS energies?

2. Light cluster production in pp and pA collisions

(9)

E. Bartsch for ALICE Collaboration, J. Phys. Conf. Ser. 1602, 012022 (2020)



CSM: V. Vovchenko et al., PLB 785, 171 (2019), PRC 100,054906 (2019)

1. Thermal model in grand canonical ensemble fails

2. Canonical statistical model (CSM) struggles (p/pi, d/p, He3/p)

$$\langle N_j^{\text{prim}} \rangle_{\text{ce}} = \frac{Z(B - B_j, Q - Q_j, S - S_j)}{Z(B, Q, S)} \langle N_j^{\text{prim}} \rangle_{\text{gce}}$$

Improvements: $T_{ch}(dN_{ch}/d\eta_{lab})$, excluded volume V_{ex} , correlation volume V_c

3. Coalescence model works (parameter free)

Coalescence:

$$\frac{N_d}{N_p} \approx \frac{4.0 \times 10^{-3}}{\left[1 + \left(\frac{1.6 \text{ fm}}{R}\right)^2\right]^{3/2}}$$

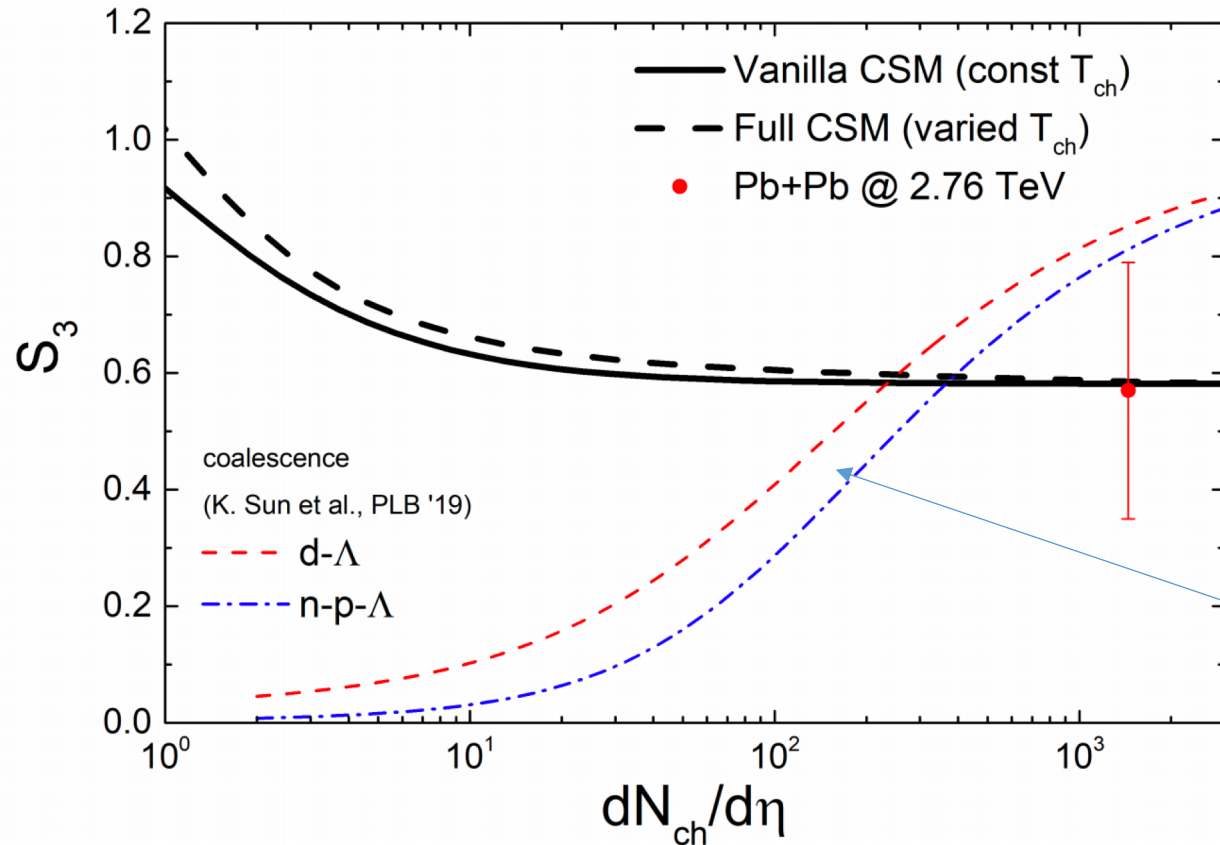
$$\frac{N_{^3\text{He}}}{N_p} \approx \frac{7.1 \times 10^{-6}}{\left[1 + \left(\frac{1.24 \text{ fm}}{R}\right)^2\right]^3}$$

$$\frac{N_{^3\text{He}}}{N_p} \approx \frac{7.1 \times 10^{-6}}{\left[1 + \left(\frac{1.15 \text{ fm}}{R}\right)^2\right]^{3/2} \left[1 + \left(\frac{1.6 \text{ fm}}{R}\right)^2\right]^{3/2}}$$

Coalescence: K. J. Sun, C. M. Ko and B. Donigus, Phys. Lett. B 792, 132 (2019)

2. Light cluster production in pp and pA collisions

(10)



Strangeness population factor:

$$S_3 = \frac{{}^3\text{H} p}{{}^3\text{He} \Lambda}$$

Coalescence model and canonical statistical model predict opposite trends

Due to the larger size of hypertriton than that of helium-3 and the emission source

A benchmark test for both models !

Figure from V. Vovchenko

3. QCD criticality on light nuclei production

[K. J. Sun, C. M. Ko, and F. Li, arXiv:2008.02325\(2020\)](#)

3. Critical phenomenon

(11)

General feature:

Scaling, universality; long-range correlation, spontaneous symmetry breaking.

In the renormalization group (RG) theory, the critical point is linked to a fixed point of RG flow

Long-range correlation leads to enhanced fluctuation:

$$(\Delta N)^2 \sim \int d\vec{r} C(\vec{r}) \sim \xi^{2-\eta}$$

Number fluc.

Density-density correlation
Correlation length

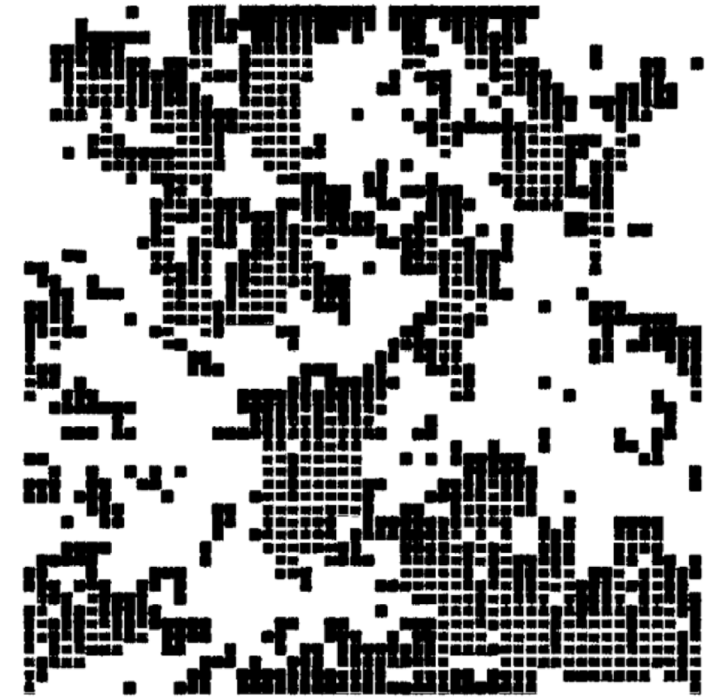
Near the critical point $C(\vec{r}) \sim \frac{e^{-r/\xi}}{r^{1+\eta}}$ with η being the anomalous dimension. $\eta \approx 0.04$ for 3d Ising model

From 'scaling and renormalization' of J. Cardy



(a)

Configuration of the Ising model at $T = T_c$



(b)

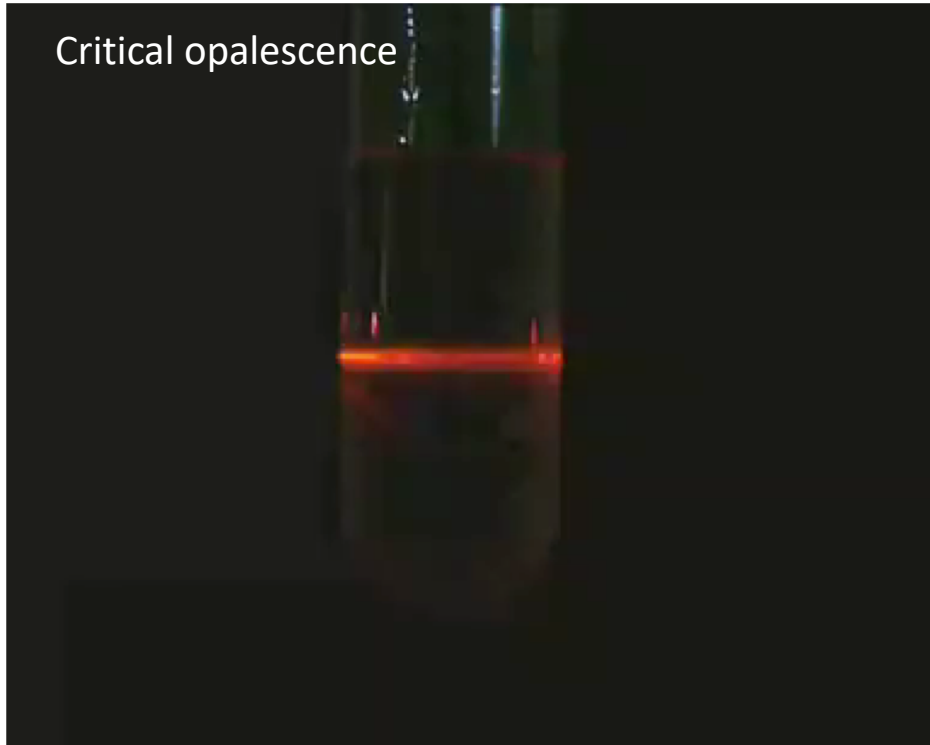
A single block spin transformation

Statistical 'clusters' of all sizes
Short-range interaction leads to long-range correlation

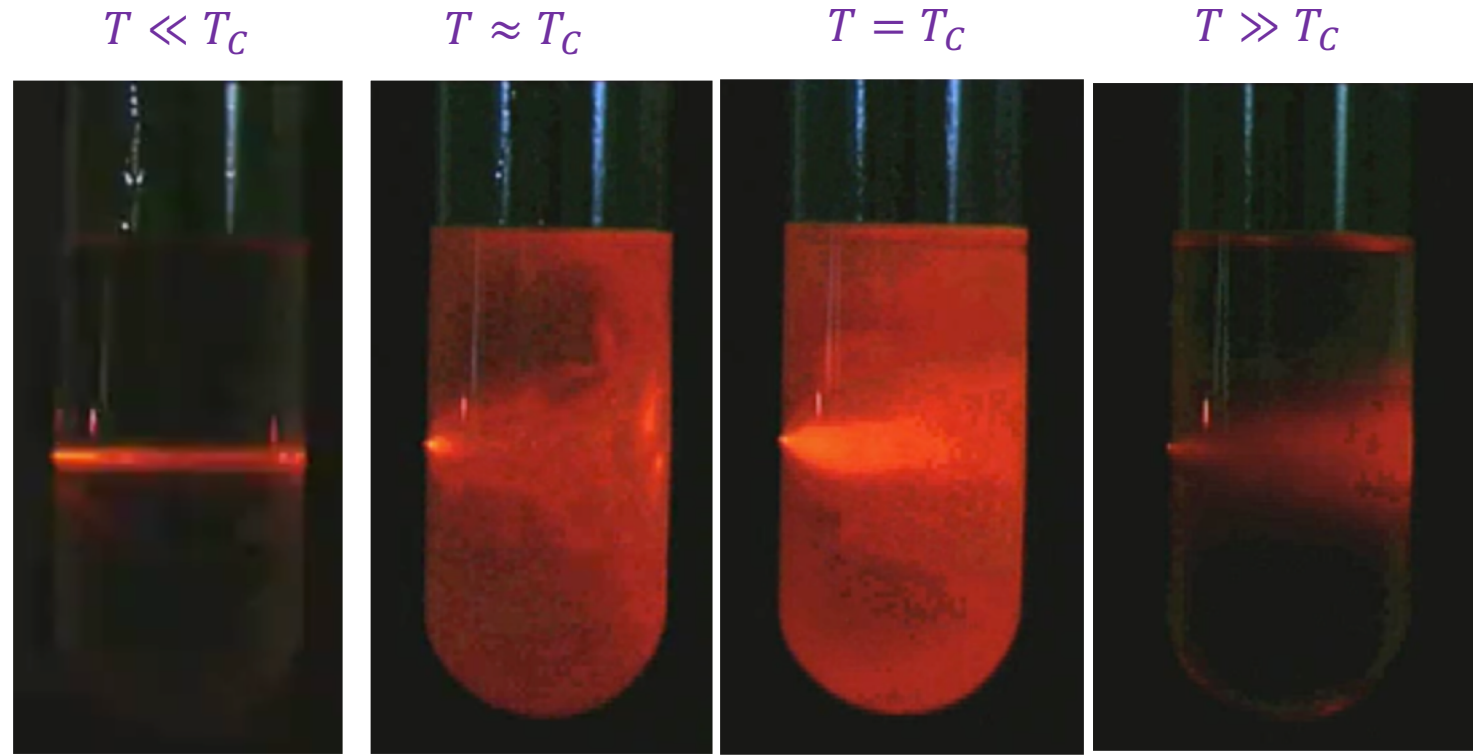
3. Critical phenomenon

(12)

Enhanced scatterings near critical point



Movie taken from <http://www.aip.org/pnu/2005/split/757-1.html>



Near the critical point:

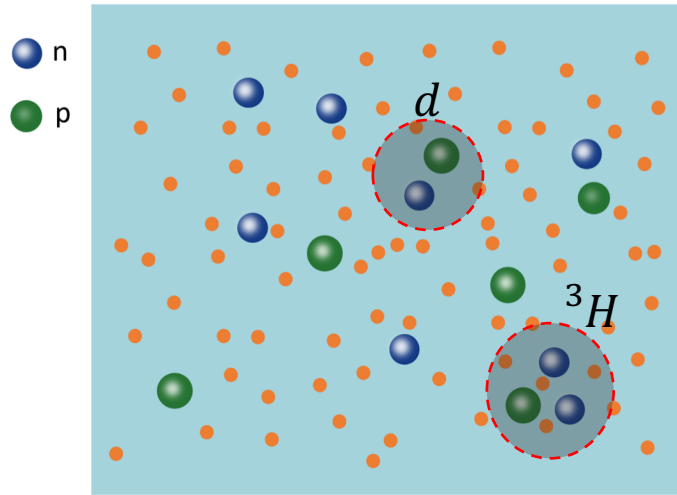
$$\underline{I} \propto \underline{S} \propto \underline{\chi_T} \sim \xi^2$$

Scattering intensity Structure function Compressibility

3. QCD criticality on light nuclei production

(13)

Consider a system in the thermal limit, i.e., $V \rightarrow \infty$, $\frac{N}{V}$ is finite. In coalescence model:



$$N_d = g_d \int dx_1 dx_2 dp_1 dp_2 f_{np}(x_1, p_1; x_2, p_2) \times W_d \left(\frac{x_1 - x_2}{\sqrt{2}}, \frac{p_1 - p_2}{\sqrt{2}} \right) g_d = \frac{3}{4}$$

Wigner function(Gaussian): $W_d(r, k) = 8 \exp \left(-\frac{r^2}{\sigma_d^2} - \sigma_d^2 k^2 \right)$ $\sigma_d \approx 2.26 \text{ fm}$

Joint distribution function: $f_{np}(x_1, p_1; x_2, p_2) \approx f_n(x_1, p_1) f_p(x_2, p_2)$

Non-relativistic: $f(x, p) \approx \rho_0 (2\pi mT)^{-\frac{3}{2}} \exp \left(-\frac{p^2}{2mT} \right)$,

$$\rho_0 = N/V = \frac{2}{(2\pi)^3} (2\pi mT)^{\frac{3}{2}} e^{\frac{\mu}{T}}, \mu = \mu_B - m$$

Flow is neglected because it has small effects on the yield (but large effects on the spectrum)

Coordinate transformation: $\vec{X} = \frac{\vec{x}_1 + \vec{x}_2}{2}$ $\vec{x} = \frac{\vec{x}_1 - \vec{x}_2}{\sqrt{2}}$ $\vec{P} = p_1 + p_2$ $\vec{p} = \frac{\vec{p}_1 - \vec{p}_2}{\sqrt{2}}$

$$\begin{aligned} N_d &\approx 8g_d \frac{N_p N_n}{(2\pi mT)^3 V^2} \int dX dx dP dp \exp \left(-\frac{\vec{P}^2}{4mT} - \frac{\vec{p}^2}{2mT} - \frac{\vec{x}^2}{\sigma_d^2} - \sigma_d^2 \vec{p}^2 \right) \\ &\approx 8g_d \frac{N_p N_n}{(2\pi mT)^3 V^2} V (4\pi mT)^{\frac{3}{2}} \left(\frac{2\pi mT}{2mT\sigma_d^2 + 1} \right)^{\frac{3}{2}} (\pi\sigma_d^2)^{\frac{3}{2}} \\ &\approx \frac{3}{\sqrt{2}} \left(\frac{2\pi}{mT} \right)^{\frac{3}{2}} \frac{N_p N_n}{V} = \frac{3V}{(2\pi)^3} (4\pi mT)^{\frac{3}{2}} e^{\frac{2\mu}{T}} \approx N_d^{th} \end{aligned}$$

Small binding energy is neglected

3. QCD criticality on light nuclei production

(14)

Similarly:

$$N_t = g_t \int dx_1 dx_2 dx_3 dp_1 dp_2 dp_3 f_{nnp}(x_1, p_1; x_2, p_2; x_3, p_3) \times W_t\left(\frac{x_1 - x_2}{\sqrt{2}}, \frac{p_1 - p_2}{\sqrt{2}}, \frac{x_1 + x_2 - 2x_3}{\sqrt{6}}, \frac{p_1 + p_2 - 2p_3}{\sqrt{6}}\right) \quad g_t = \frac{1}{4}$$

Wigner function: $W_t(\rho, \lambda, k_\rho, k_\lambda) = 8^2 \exp\left(-\frac{\rho^2}{\sigma_t^2} - \frac{\lambda^2}{\sigma_t^2} - \sigma_t^2 k_\rho^2 - \sigma_t^2 k_\lambda^2\right) \quad \sigma_t \approx 1.59 \text{ fm}$

$$f_{nnp}(x_1, p_1; x_2, p_2; x_3, p_3) = f_n(x_1, p_1) f_n(x_2, p_2) f_p(x_3, p_3)$$

Coordinate transformation:

$$X = \frac{x_1 + x_2 + x_3}{3} \quad x = \frac{x_1 - x_2}{\sqrt{2}} \quad \lambda = \frac{x_1 + x_2 - 2x_3}{\sqrt{6}}$$

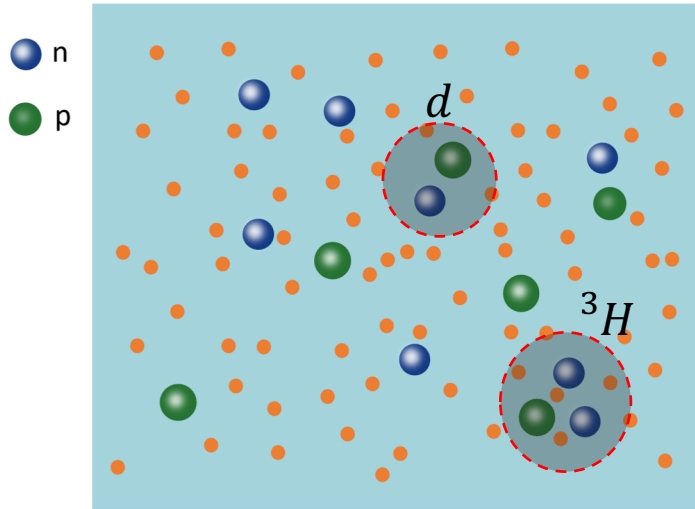
$$P = \frac{p_1 + p_2 + p_3}{3} \quad p = \frac{p_1 - p_2}{\sqrt{2}} \quad p_\lambda = \frac{p_1 + p_2 - p_3}{\sqrt{6}}$$

$$\longrightarrow N_t \approx \frac{3^{\frac{3}{2}}}{4} \left(\frac{2\pi}{mT}\right)^3 \frac{N_p N_n^2}{V^2} \approx N_t^{th}$$

$$\longrightarrow \frac{N_t N_p}{N_d^2} \approx \frac{1}{2\sqrt{3}}$$

3. QCD criticality on light nuclei production

(15)



Include density fluctuation and correlation:

$$f_{np}(x_1, p_1; x_2, p_2) = \rho_{np}(x_1, x_2)(2\pi mT)^{-3} e^{-\frac{p_1^2 + p_2^2}{2mT}}$$

$$\rho_{np}(x_1, x_2) = \rho_n(x_1)\rho_p(x_2) + C_2(x_1, x_2)$$

$$\rho_n(x) = \langle \rho_n \rangle + \delta\rho_n(x) \quad \rho_p(x) = \langle \rho_p \rangle + \delta\rho_p(x) \quad \langle \dots \rangle \equiv \frac{1}{V} \int dx$$

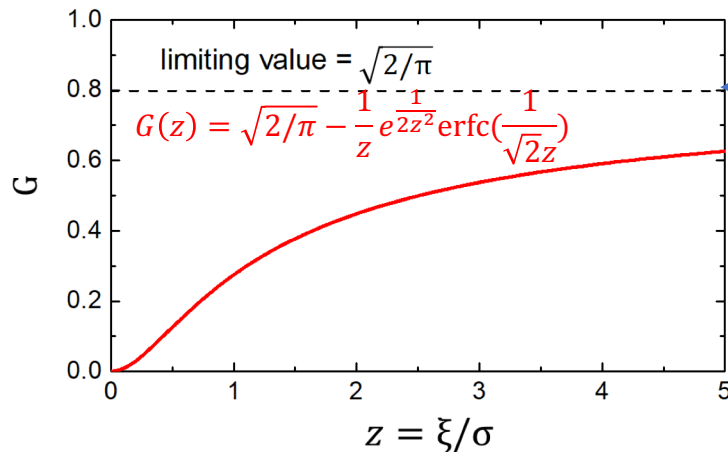
$\delta\rho(x)$ denotes density fluctuation over space or inhomogeneity,

this term will be important when a first-order phase transition takes place.

$$C_2(x_1 - x_2) \approx \lambda \langle \rho_n \rangle \langle \rho_p \rangle \frac{e^{-|x_1 - x_2|/\xi}}{|x_1 - x_2|^{1+\eta}} \quad (\text{singular part only})$$

with ξ being the density – density correlation length

$$0 < \langle \delta N^2 \rangle \sim \int dx C_2(x) \sim \lambda \xi^2 \rightarrow \lambda > 0$$



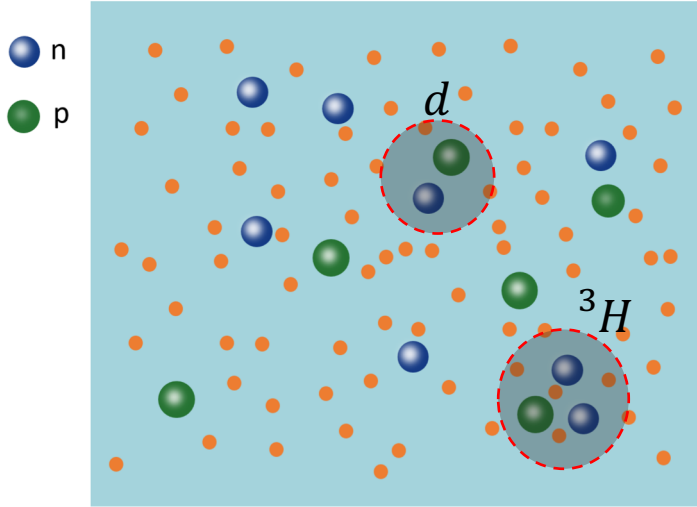
$$N_d \approx \frac{3}{\sqrt{2}} \left(\frac{2\pi}{mT}\right)^{\frac{3}{2}} N_p \langle \rho_n \rangle \left[1 + C_{np} + \frac{\lambda}{\sigma_d} G\left(\frac{\xi}{\sigma_d}\right) \right]$$

$$C_{np} = \frac{\langle \delta\rho_n(x)\delta\rho_p(x) \rangle}{\langle \rho_n \rangle \langle \rho_p \rangle}$$

$$\Delta\rho_n = \frac{\langle \delta\rho_n(x)^2 \rangle}{\langle \rho_n \rangle^2}$$

3. QCD criticality on light nuclei production

(16)

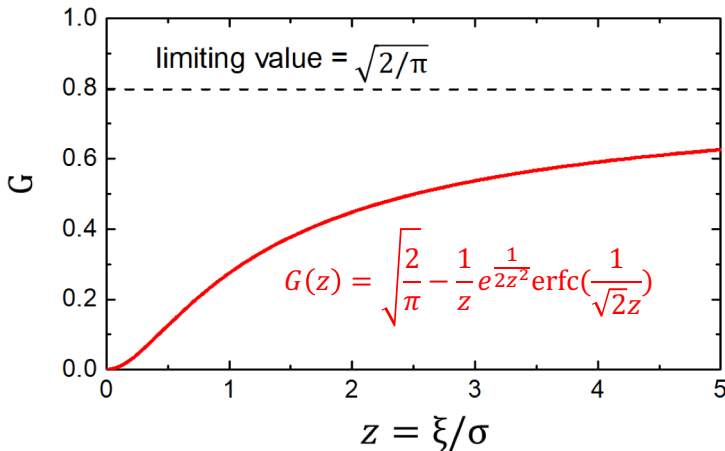


Joint distribution function in phase space:

$$f_{nnp}(x_1, p_1; x_2, p_2; x_3, p_3) = \rho_{nnp}(x_1, x_2, x_3) (2\pi mT)^{-\frac{9}{2}} e^{-\frac{p_1^2 + p_2^2 + p_3^2}{2mT}}$$

$$\rho_{nnp}(x_1, x_2, x_3) = \rho_n(x_1)\rho_n(x_2)\rho_p(x_3) + \rho_n(x_1)C_2(x_2, x_3) + \rho_n(x_2)C_2(x_1, x_3) + \rho_p(x_3)C_2(x_1, x_2) + C_3(x_1, x_2, x_3)$$

$$C_3(x_1, x_2, x_3) \sim \frac{\lambda' \langle \rho_n \rangle^2 \langle \rho_p \rangle e^{-\frac{|x_1 - x_2| + |x_2 - x_3|}{\xi}}}{|x_1 - x_2| |x_2 - x_3|} + (1 \rightarrow 2, 2 \rightarrow 3) + (1 \rightarrow 3, 2 \rightarrow 1)$$

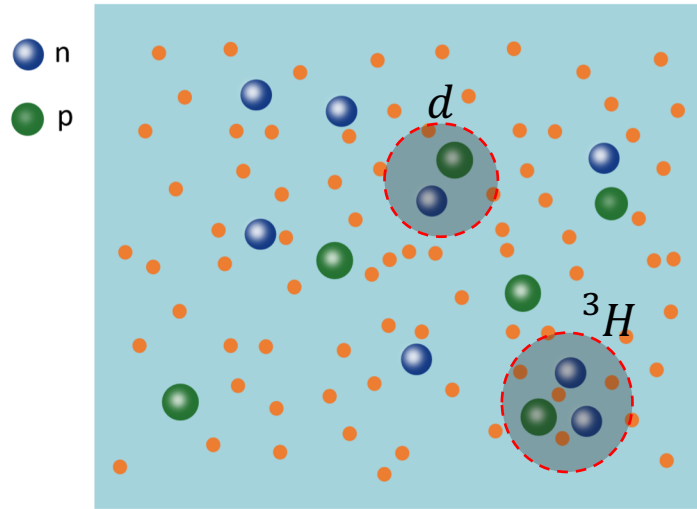


$$N_t \approx \frac{3^{3/2}}{4} \left(\frac{2\pi}{mT}\right)^3 N_p \langle \rho_n \rangle^2 [1 + 2C_{np} + \Delta\rho_n + \frac{3\lambda}{\sigma_d} G\left(\frac{\xi}{\sigma_t}\right) + O(G^2)]$$

$$\begin{aligned} \rho_n(x) &= \langle \rho_n \rangle + \delta\rho_n(x) & C_{np} &= \frac{\langle \delta\rho_n(x)\delta\rho_p(x) \rangle}{(\langle \rho_n \rangle \langle \rho_p \rangle)} \\ \rho_p(x) &= \langle \rho_p \rangle + \delta\rho_p(x) & \Delta\rho_n &= \frac{\langle \delta\rho_n(x)^2 \rangle}{\langle \rho_n \rangle^2} \end{aligned}$$

3. QCD criticality on light nuclei production

(17)



$$N_d = \frac{3}{\sqrt{2}} \left(\frac{2\pi}{mT} \right)^{\frac{3}{2}} N_p \langle \rho_n \rangle \left[1 + C_{np} + \frac{\lambda}{\sigma_d} G\left(\frac{\xi}{\sigma_d}\right) \right]$$

$$N_t = \frac{3^{3/2}}{4} \left(\frac{2\pi}{mT} \right)^3 N_p \langle \rho_n \rangle^2 \left[1 + 2C_{np} + \Delta\rho_n + \frac{3\lambda}{\sigma_d} G\left(\frac{\xi}{\sigma_d}\right) + O(G^2) \right]$$

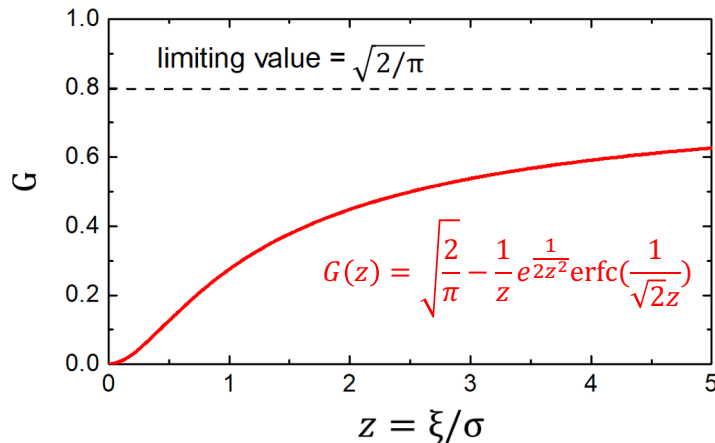
Pre-factors are thermal yields w/o density fluc./corr.
To see fine structures:

Ratio: $\frac{N_t N_p}{N_d^2} \approx \frac{1}{2\sqrt{3}} \left[1 + \Delta\rho_n + \frac{\lambda}{\sigma} G\left(\frac{\xi}{\sigma}\right) \right], \quad \frac{3 \text{ pairs}}{2 \text{ pairs}} \sim 1 \text{ pair}, \quad \sigma \approx 2 \text{ fm}$

1. Enhancement of ξ leads to enhancement of tp/d^2
2. The function G doesn't explode when $\xi \rightarrow \infty$
3. A novel phenomenon of criticality similar to but different from the critical opalescence!

Heavier nucleus:

$$\frac{N_\alpha N_p}{N_{3\text{He}} N_d} \approx \frac{2\sqrt{2}}{9\sqrt{3}} \left[1 + C_{np} + \Delta\rho_n + \frac{2\lambda}{\sigma} G\left(\frac{\xi}{\sigma}\right) \right] \quad \frac{N_\alpha N_t N_p^2}{N_{3\text{He}} N_d^3} \approx \frac{1}{27\sqrt{2}} \left[1 + C_{np} + 2\Delta\rho_n + \frac{3\lambda}{\sigma} G\left(\frac{\xi}{\sigma}\right) \right]$$



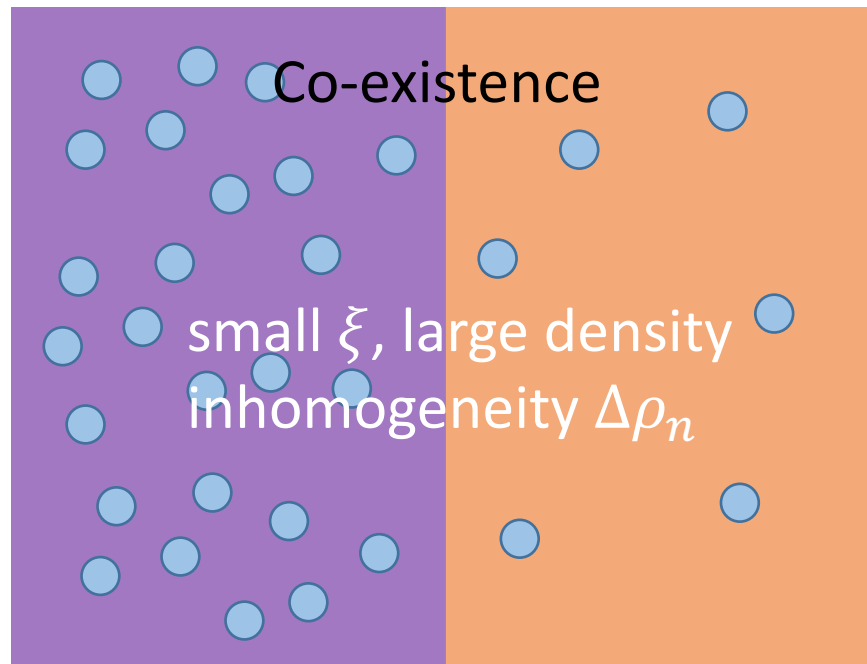
3. QCD criticality on light nuclei production

(18)

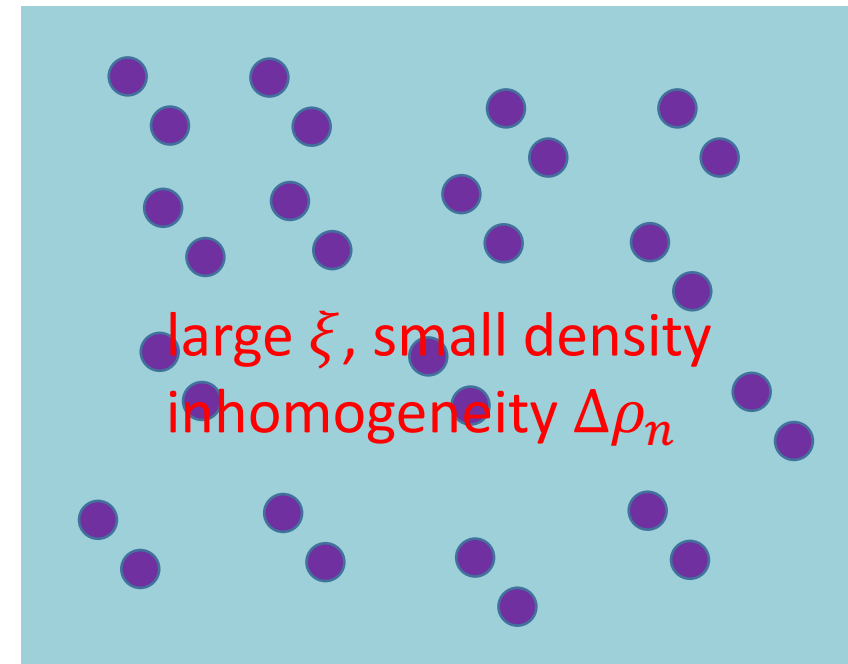
$$\frac{N_t N_p}{N_d^2} \approx \frac{1}{2\sqrt{3}} \left[1 + \Delta\rho_n + \frac{\lambda}{\sigma} G\left(\frac{\xi}{\sigma}\right) \right]$$

First-order phase transition

Phase I: ρ_I Phase II: ρ_{II}



Second-order phase transition



3. QCD criticality on light nuclei production

Near critical point:

$$\frac{(\Delta N)^2}{\text{Number fluc.}} \sim \int d\vec{r} \underbrace{C(\vec{r})}_{\text{Density-density correlation}} \sim \underbrace{\xi^2}_{\text{Correlation length}}$$

$$\underbrace{I}_{\text{Scattering intensity}} \propto \underbrace{S}_{\text{Structure function}} \propto \underbrace{\chi_T}_{\text{Compressibility}} \sim \xi^2$$

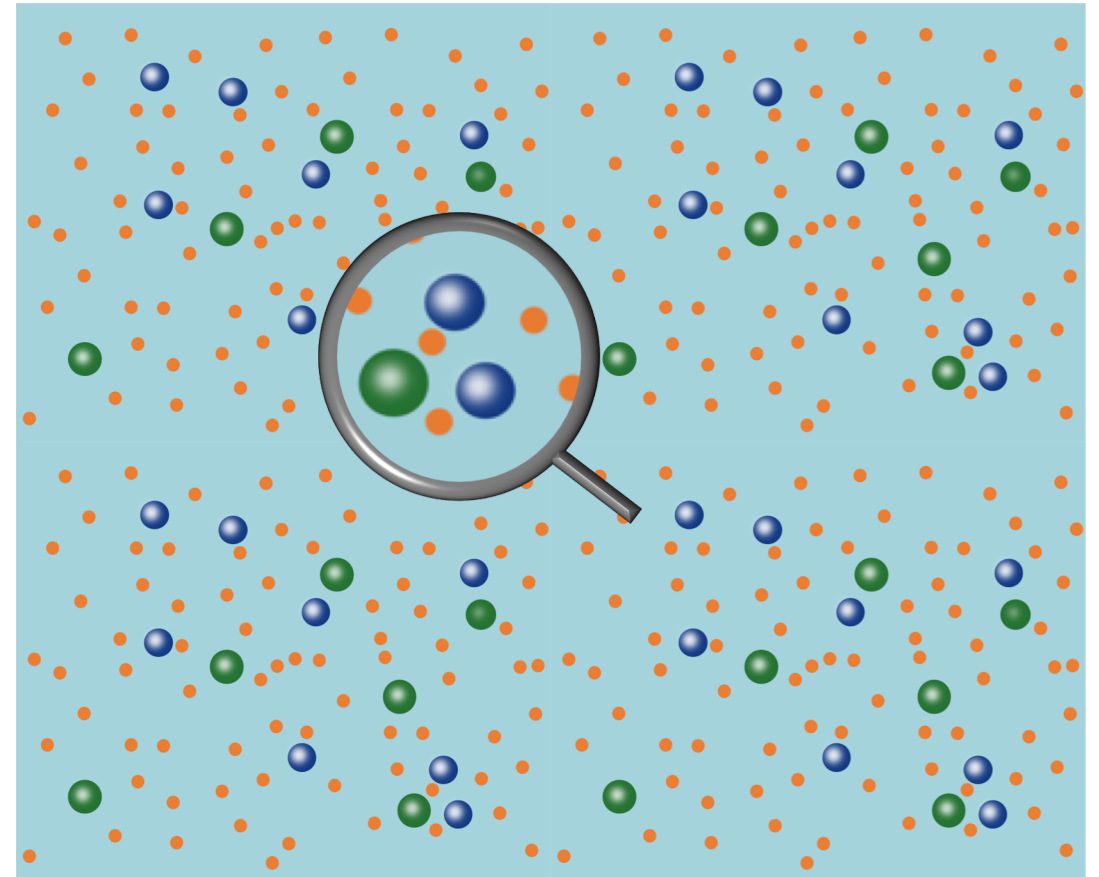
New phenomenon:

$$\frac{N_t N_p}{N_d^2} \approx \frac{1}{2\sqrt{3}} \left[1 + \Delta\rho_n + \frac{\lambda}{\sigma} G\left(\frac{\xi}{\sigma}\right) \right]$$

An unique feature:

The size of light nuclei provides a natural **resolution scale** σ as small as 2 fm which is comparable to the correlation length ξ that can be generated in realistic heavy-ion collisions near the CEP.

The light nucleus (d, t), like a microscope, allows us to observe the density inhomogeneity as well as the long-range correlation.



3. QCD criticality on light nuclei production

(20)

$$\frac{N_t N_p}{N_d^2} \approx \frac{1}{2\sqrt{3}} \left[1 + \underline{\Delta\rho_n} + \frac{\lambda}{\sigma} G\left(\frac{\xi}{\sigma}\right) \right]$$

In thermal model, assuming nucleon chemical potential depends on spatial coordinates

$$\begin{aligned} \rho_{n,p}(\mathbf{x}) &= \frac{2}{(2\pi)^3} 4\pi T m^2 K_2\left(\frac{m}{T}\right) e^{\frac{\mu_{n,p}(\mathbf{x})}{T}} \\ \rho_d(\mathbf{x}) &= \frac{3}{(2\pi)^3} 4\pi T (2m)^2 K_2\left(\frac{2m}{T}\right) e^{\frac{\mu_n(\mathbf{x}) + \mu_p(\mathbf{x})}{T}} \\ \rho_t(\mathbf{x}) &= \frac{2}{(2\pi)^3} 4\pi T (3m)^2 K_2\left(\frac{3m}{T}\right) e^{\frac{2\mu_n(\mathbf{x}) + \mu_p(\mathbf{x})}{T}} \end{aligned}$$

$$\begin{aligned} \longrightarrow \frac{N_t N_p}{N_d^2} &= \frac{K_2\left(\frac{m}{T}\right) K_2\left(\frac{3m}{T}\right)}{4\left(K_2\left(\frac{2m}{T}\right)\right)^2} \frac{\int d^3\mathbf{x} \rho_p \int d^3\mathbf{x} \rho_n^2 \rho_p}{\left[\int d^3\mathbf{x} \rho_n \rho_p\right]^2} \\ &\approx \frac{1}{2\sqrt{3}} \frac{\int d^3\mathbf{x} \rho_p \int d^3\mathbf{x} \rho_n^2 \rho_p}{\left[\int d^3\mathbf{x} \rho_n \rho_p\right]^2} \end{aligned}$$

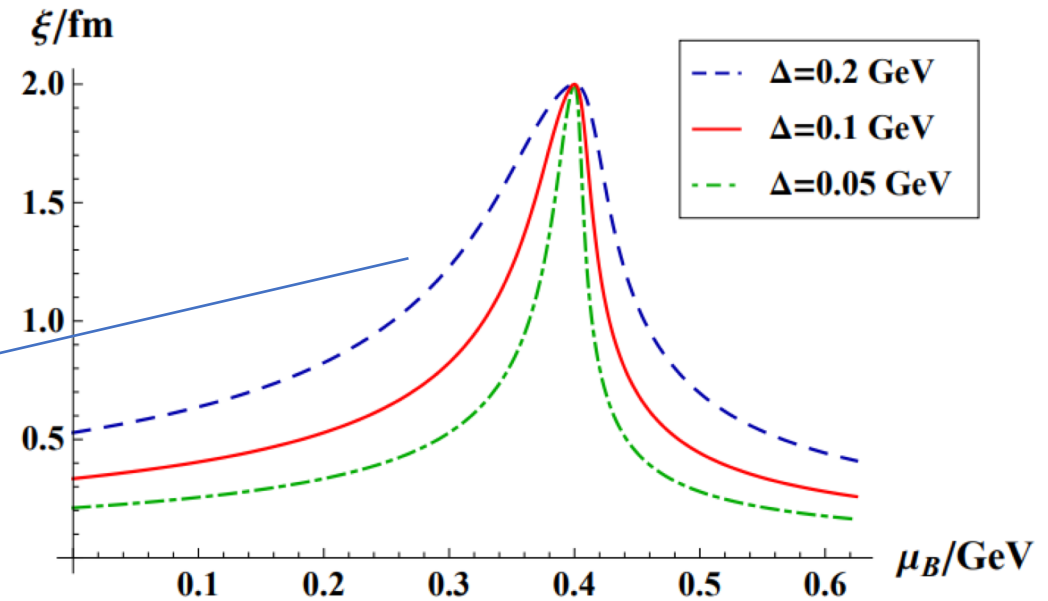
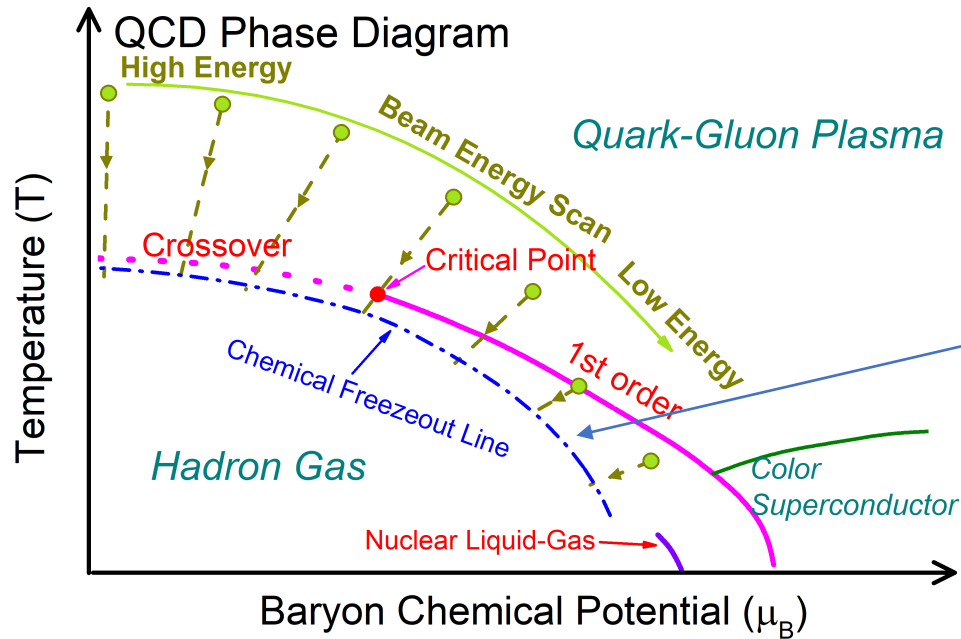
$$\longrightarrow \frac{N_t N_p}{N_d^2} \approx \frac{1}{2\sqrt{3}} [1 + \Delta\rho_n]$$

3. Enhancement of tp/d^2 near the critical point

(21)

$$\frac{N_t N_p}{N_d^2} \approx \frac{1}{2\sqrt{3}} \left[1 + \Delta\rho_n + \frac{\lambda}{\sigma} G\left(\frac{\xi}{\sigma}\right) \right]$$

C. Athanasion, K. Rajagopal, and M. Stephanov, Phys. Rev. D82, 074008 (2010)



$$\xi(\mu_B) = \frac{\xi_{max}}{\left[1 + \frac{(\mu_B - \mu_B^c)^2}{W(\mu_B)^2} \right]^{1/3}}$$

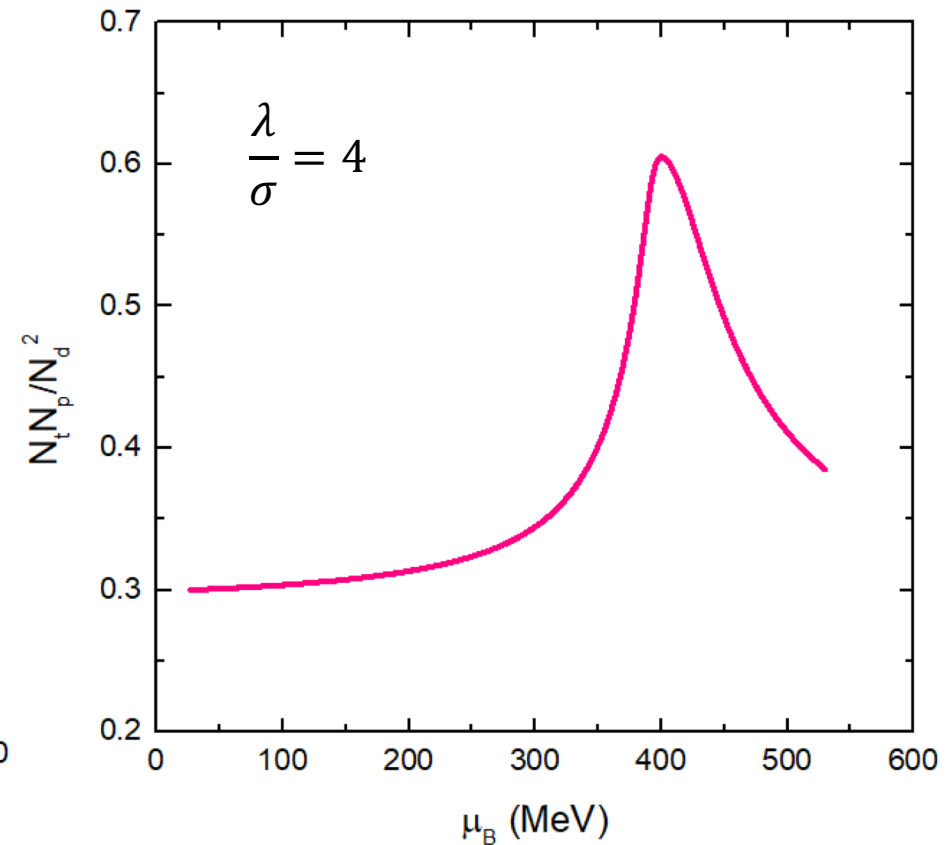
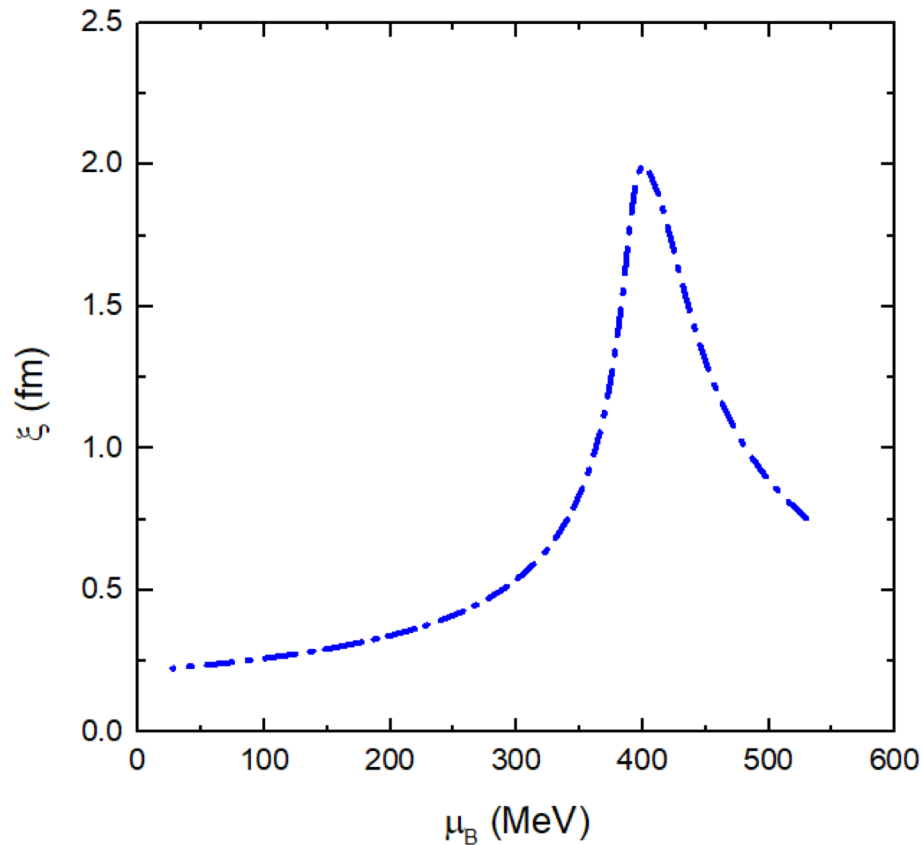
$$W(\mu_B) = W + \delta W \tanh\left(\frac{\mu_B - \mu_B^c}{w}\right) \quad W \approx 2.2 \delta W$$

Peak of ξ near the critical point

3. Enhancement of tp/d^2 near the critical point

(22)

$$\frac{N_t N_p}{N_d^2} \approx \frac{1}{2\sqrt{3}} \left[1 + \Delta\rho_n + \frac{\lambda}{\sigma} G\left(\frac{\xi}{\sigma}\right) \right] \quad G(z) = \sqrt{\frac{2}{\pi}} - \frac{1}{z} e^{\frac{1}{2z^2}} \operatorname{erfc}\left(\frac{1}{\sqrt{2}z}\right)$$



Peak of ξ leads to peak of tp/d^2

3. Baryon clustering near the QCD critical point

(23)

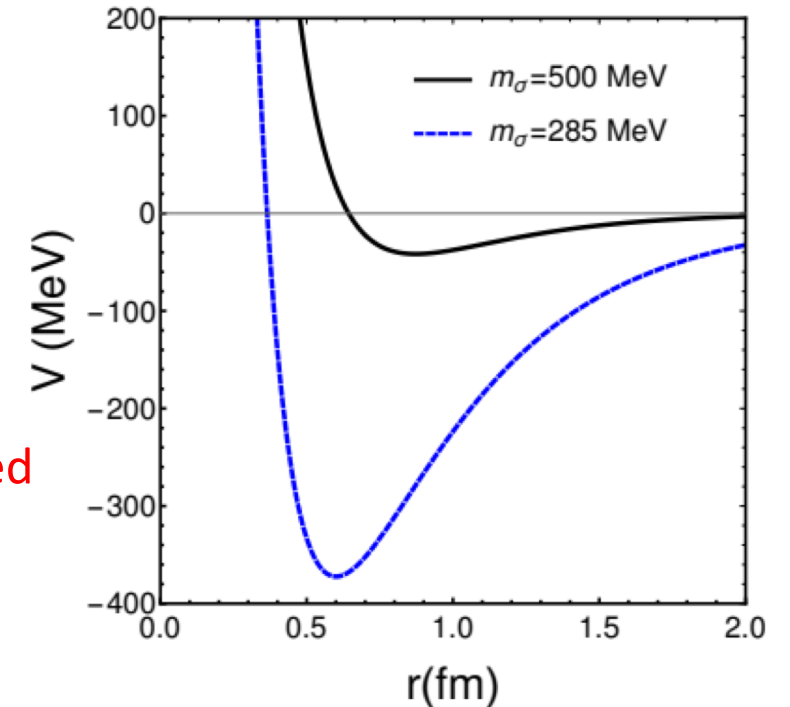
Nucleon-Nucleon potential:

$$V_A(r) = -\frac{g_\sigma^2}{4\pi r} e^{-m_\sigma r} + \frac{g_\omega^2}{4\pi r} e^{-m_\omega r}$$

$$g_\sigma^2 = 267.1 \left(\frac{m_\sigma^2}{m_N^2} \right), \quad g_\omega^2 = 195.9 \left(\frac{m_\omega^2}{m_N^2} \right)$$

Near the critical point, the mass of sigma meson ($m_\sigma \sim 1/\xi$) is reduced

1. Precluster formation is related to $\exp(-V(r_{min})/T)$, thus the modified NN potential leads to stronger baryon clustering.
2. Preclusters decay into bound nuclei which are observed in experiments.



$$\mathcal{O}_{tpd} \simeq 0.29 \frac{\langle e^{-3V/T} \rangle}{\langle e^{-V/T} \rangle^2} \quad \mathcal{O}_{\alpha p^3 \text{Hed}} \equiv \frac{N_\alpha N_p}{N_{3\text{He}} N_d} \simeq 0.18 \frac{\langle e^{-6V/T} \rangle}{\langle e^{-3V/T} \rangle \langle e^{-V/T} \rangle} \quad \mathcal{O}_{\alpha tp^3 \text{Hed}} \equiv \frac{N_\alpha N_t N_p^2}{N_{3\text{He}} N_d^3} \simeq 0.05 \frac{\langle e^{-6V/T} \rangle}{\langle e^{-V/T} \rangle^3}$$

In the thermal model, modified NN potential leads to. larger binding energy, thus large yields of light nuclei. Multi-body interactions suppress clustering, see [D. DeMartini and E. Shuryak, arXiv:2010.02785]

Note: 1. In NJL model or linear sigma model, when $\xi \rightarrow \infty$, $m_\sigma \approx 2m_q$ remains finite at the CEP.

2. The modified potential quickly restores to its normal value when system moves away from the CEP

4. Effects of first-order chiral phase transition on light nuclei production within a transport approach

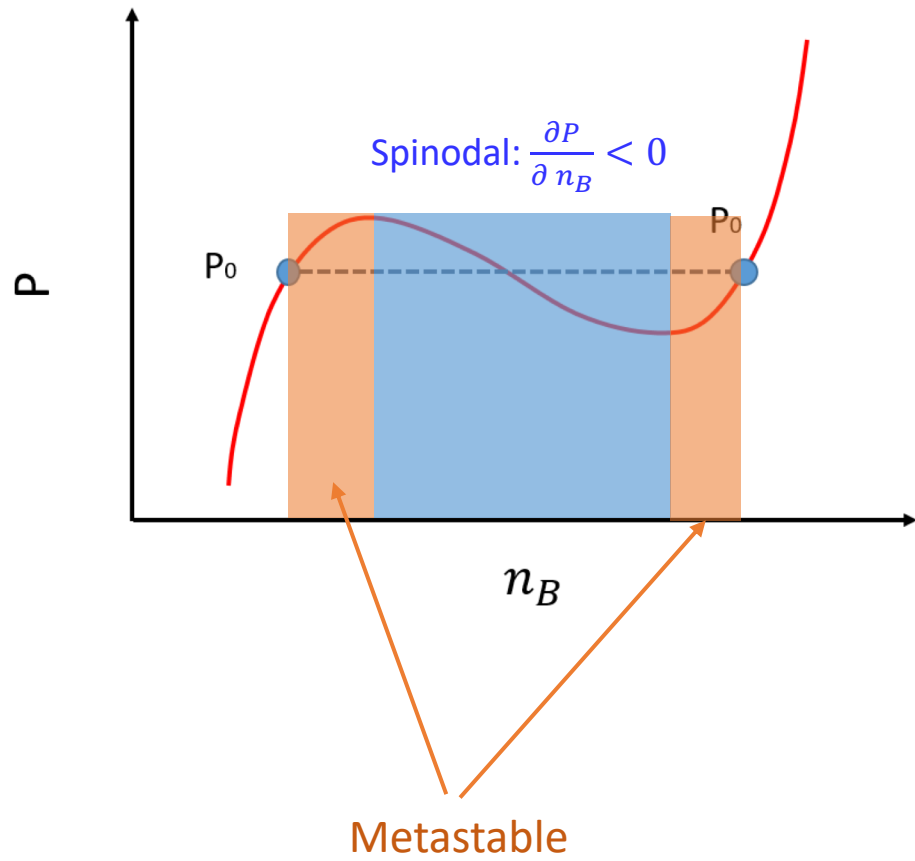
K. J. Sun, C. M. Ko, F. Li, J. Xu, and L. W. Chen, arXiv:2006.08929(2020)

$$\frac{N_t N_p}{N_d^2} \approx \frac{1}{2\sqrt{3}} \left[1 + \Delta\rho_n + \frac{\lambda}{\sigma} G\left(\frac{\xi}{\sigma}\right) \right]$$

4. First-order phase transition

(24)

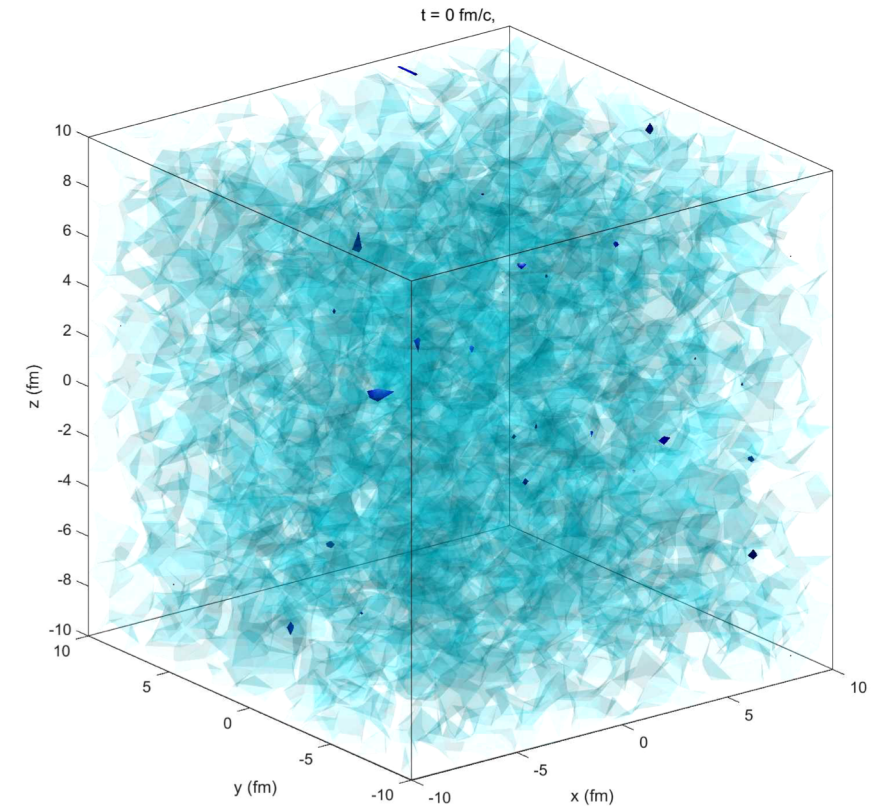
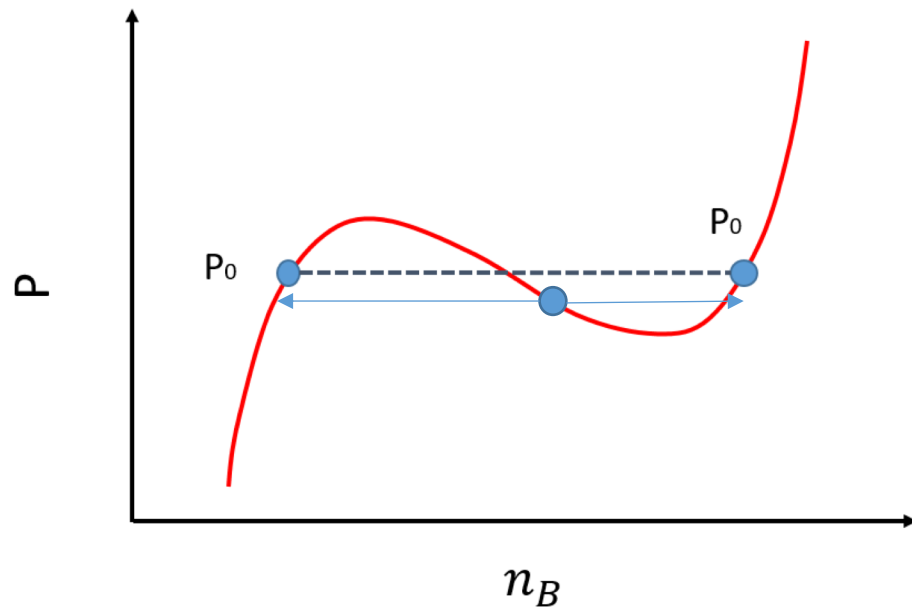
Phase separation, spinodal decomposition(SD)



4. First-order phase transition

(24)

Phase separation, spinodal decomposition(SD)



Small irregularities will grow exponentially and soon the evolution becomes 'chaotic'.

In low-energy nuclear reactions, SD could lead to nuclear multifragmentation

(P. Chomaz, M. Clonna, and J. Randrup, Phys. Rep. 389, 263 (2004)).

Q: Whether the large density fluctuation/inhomogeneity can survive the fireball expansion?

Hydro: J. Steinheimer and J. Randrup, PRL. 109, 212301 (2012); PRC79, 054911 (2009); K. Paech, A. Dumitru, PLB623, 200 (2005)

Chiral Fluid Dynamics: C. Herold, M. Nahrgang, I. Mishustin, and M. Bleicher, NPA 925, 14 (2014)

Transport: F. Li and C. M. Ko, PRC95, 055203 (2017); K. J. Sun et al., arXiv:2006.08929(2020)

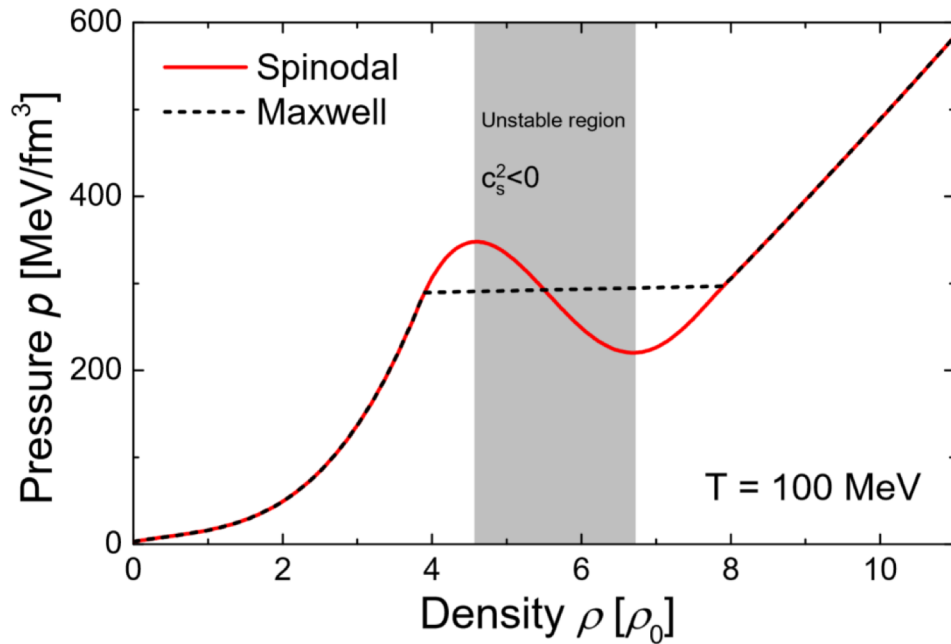
4. Short review

(25)

Hydrodynamics

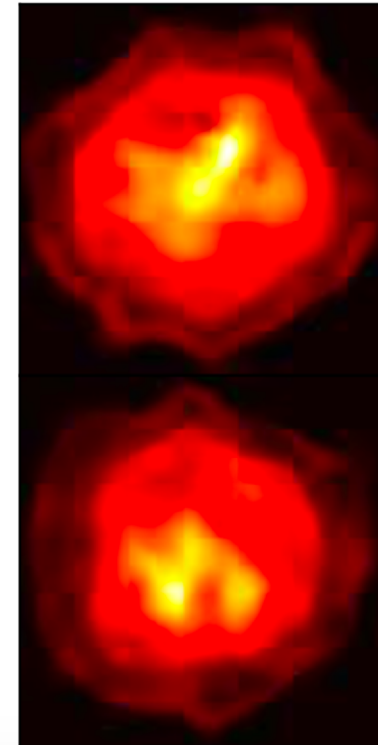
$$\partial_\mu T^{\mu\nu} = 0 \quad \partial_\mu j^\mu = 0$$

$$p(\mathbf{r}) = p_0(\varepsilon(\mathbf{r}), \rho(\mathbf{r})) - a^2 \frac{\varepsilon_s}{\rho_s^2} \rho(\mathbf{r}) \nabla^2 \rho(\mathbf{r})$$

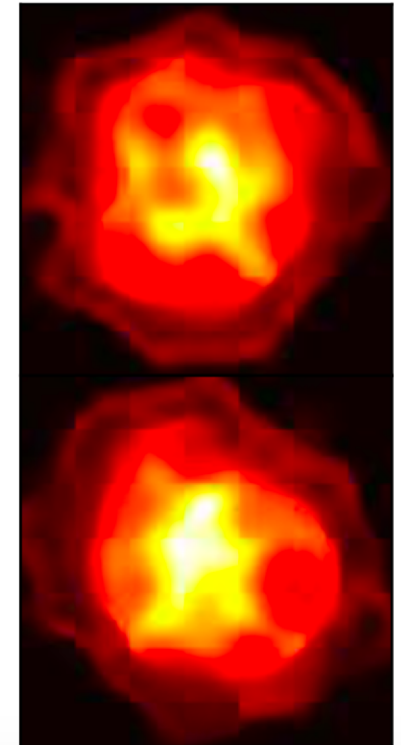


Density profile in coordinate space

Spinodal



Maxwell



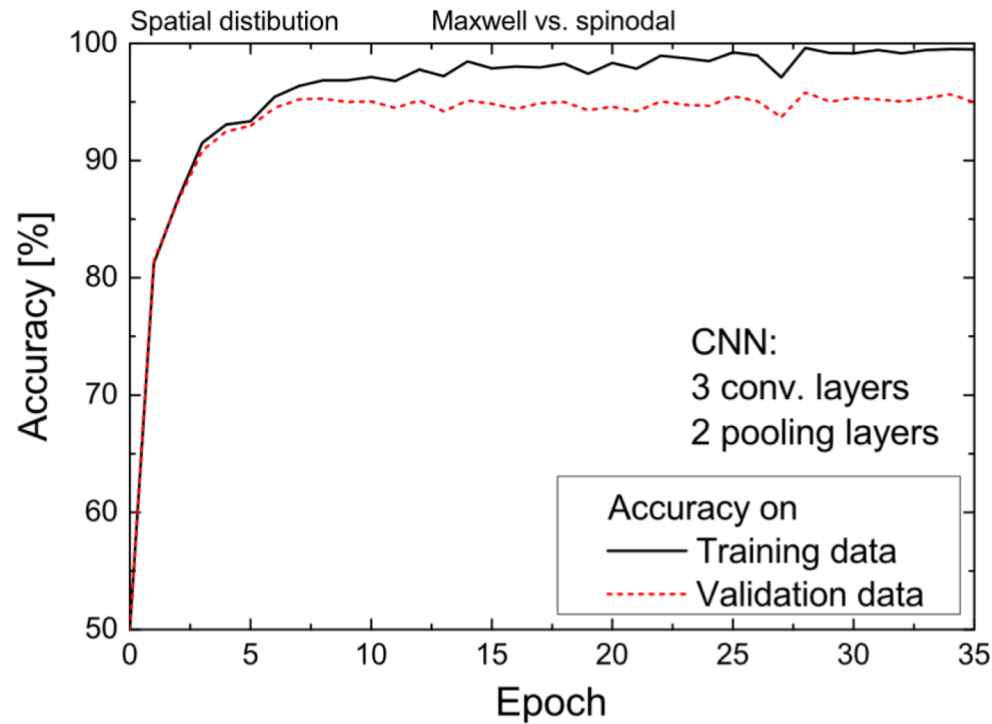
At the time of largest density fluct.

J. Steinheimer and J. Randrup, Phys. Rev. Lett. 109, 212301 (2012)

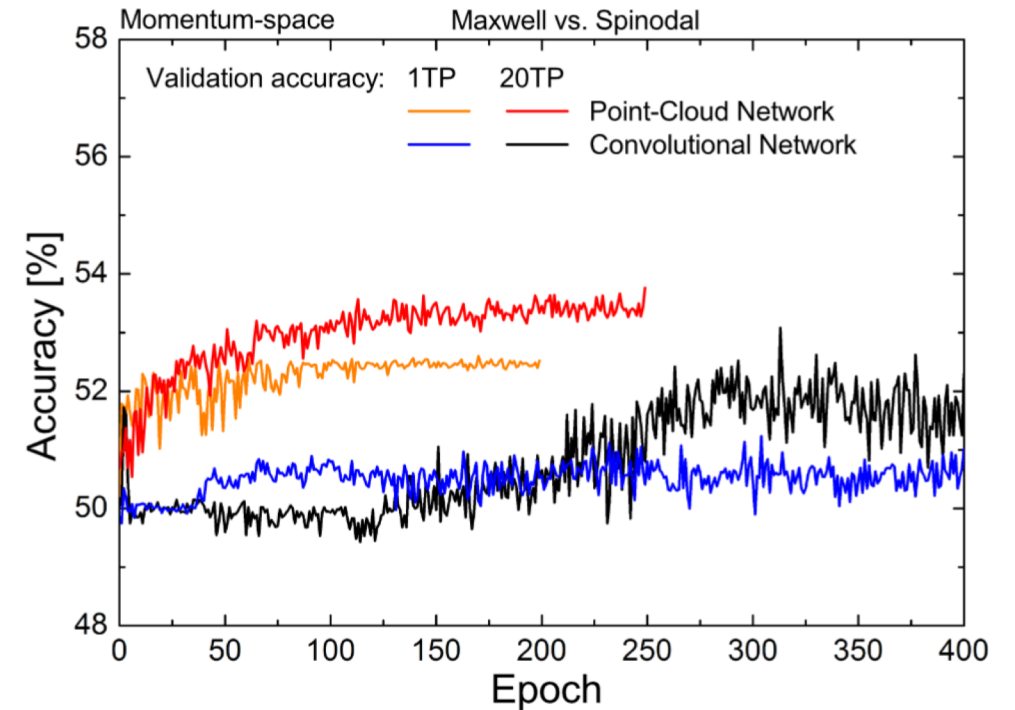
J. Steinheimer et al., JHEP 12, 122 (2019)

Machine learning

J. Steinheimer et al., JHEP 12, 122 (2019)



Coordinate space
succeed



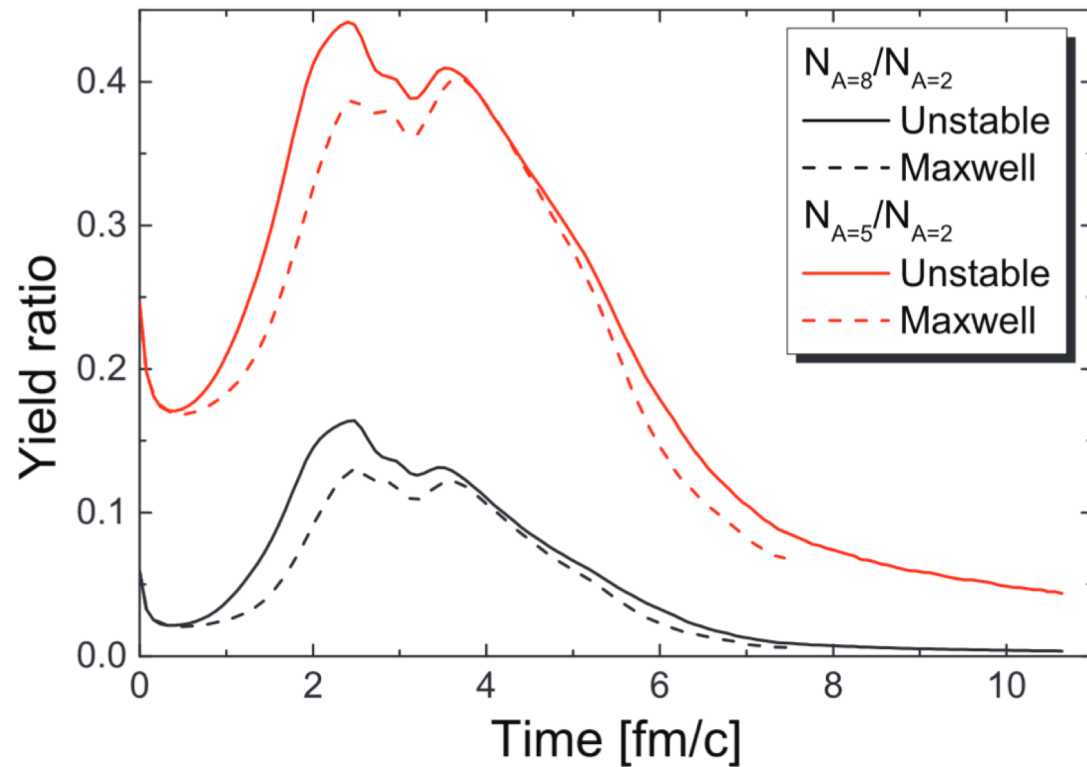
Momentum space
fail

Significant difference in coordinate space, nearly no difference in momentum space

4. Short review

Steinheimer et al., Phys. Rev. C89, 034901 (2014)

Hydrodynamics



$$N_A = \int d^3 \mathbf{p} d^3 \mathbf{r} f_A(\mathbf{r}, \mathbf{p})$$
$$f_A(\mathbf{r}, \mathbf{p}) \propto \exp[-(\sqrt{m_A^2 + p^2} - \mu_A(\mathbf{r}))/T(\mathbf{r})]$$

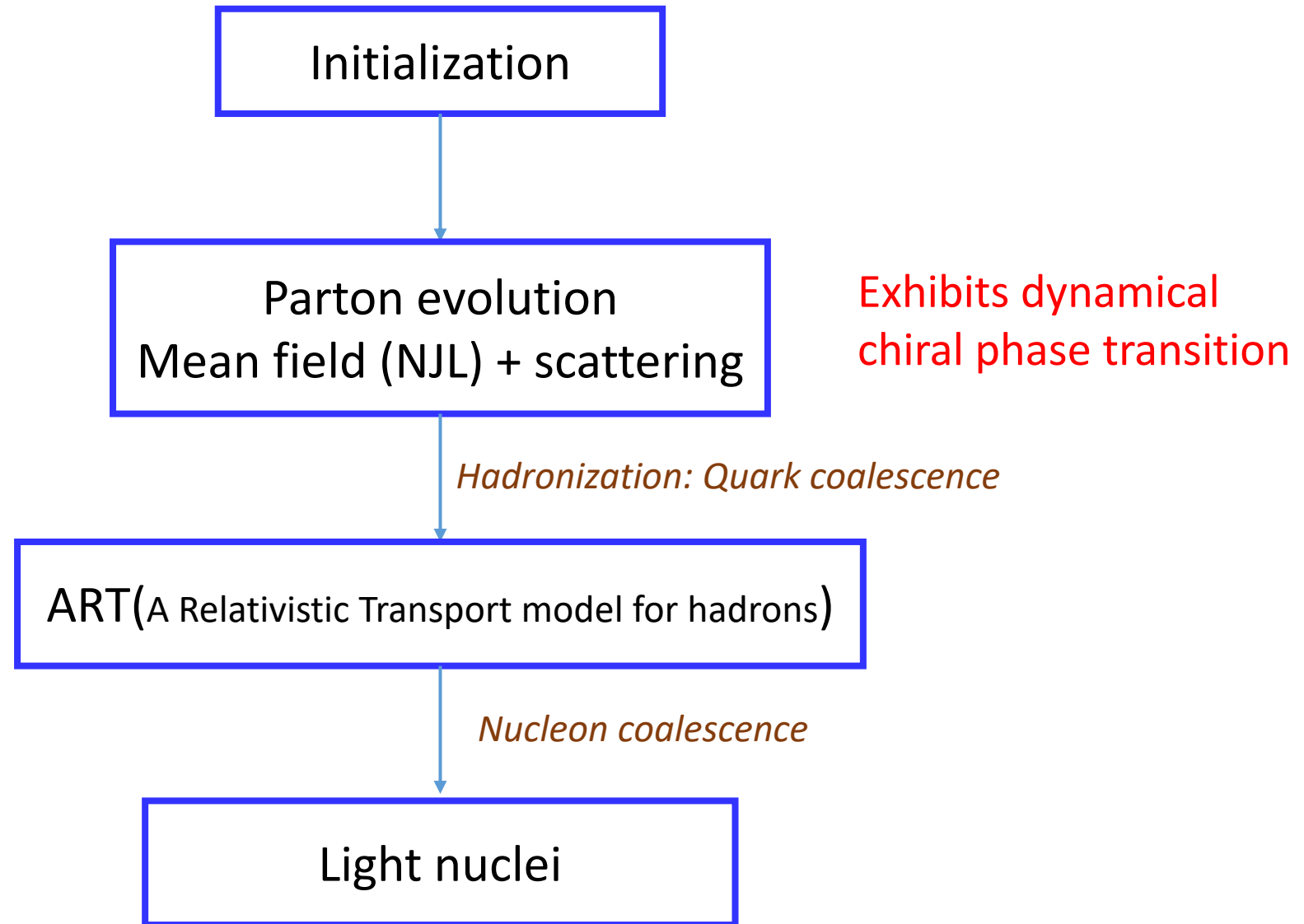
Less than 20% effect

To test



4. Framework

(28)



4. Partonic interaction and equation of state

We adopt the Nambu-Jona-Lasino (NJL) model to describe the partonic interaction at finite μ_B . This model was originally proposed in terms of nucleon degree of freedom to explain nucleon mass based on an analogy between the Dirac equation and the gap equation in BCS theory for superconductivity .

3-flavor NJL model:

$$\mathcal{L} = \mathcal{L}_0 + \mathcal{L}_S + \mathcal{L}_V + \mathcal{L}_{\text{det}},$$

with

$$\mathcal{L}_0 = \bar{\psi}(i\gamma^\mu\partial_\mu - \hat{m})\psi,$$

$$\mathcal{L}_S = G_S \sum_{a=0}^8 [(\bar{\psi}\lambda^a\psi)^2 + (\bar{\psi}i\gamma_5\lambda^a\psi)^2],$$

$$\mathcal{L}_V = -g_V(\bar{\psi}\gamma^\mu\psi)^2,$$

$$\mathcal{L}_{\text{det}} = -K[\det\bar{\psi}(1 + \gamma_5)\psi + \det\bar{\psi}(1 - \gamma_5)\psi]$$

Λ [MeV]	602.3	$M_{u,d}$ [MeV]	367.7
$G\Lambda^2$	1.835	M_s [MeV]	549.5
$K\Lambda^5$	12.36	$\langle(\bar{u}u)\rangle^{1/3}$ [MeV]	-241.9
$m_{u,d}$ [MeV]	5.5	$\langle(\bar{s}s)\rangle^{1/3}$ [MeV]	-257.7
m_s [MeV]	140.7		

Mean-field approximation

$$\begin{aligned} \mathcal{L} = & \bar{u}(\gamma^\mu iD_{u\mu} - M_u)u + \bar{d}(\gamma^\mu iD_{d\mu} - M_d)d \\ & + \bar{s}(\gamma^\mu iD_{s\mu} - M_s)s - 2G_S(\phi_u^2 + \phi_d^2 + \phi_s^2) \\ & + 4K\phi_u\phi_d\phi_s + g_V(j_u^\mu + j_d^\mu + j_s^\mu)(j_{u\mu} + j_{d\mu} + j_{s\mu}) \end{aligned}$$

$$iD_{u\mu} = i\partial_\mu - A_{u\mu}, \quad iD_{d\mu} = i\partial_\mu - A_{d\mu},$$

$$iD_{s\mu} = i\partial_\mu - A_{s\mu},$$

$$A_{u\mu} = A_{d\mu} = A_{s\mu} = 2g_V(j_{u\mu} + j_{d\mu} + j_{s\mu})$$

Effective mass:

$$M_u = m_u - 4G_S\phi_u + 2K\phi_d\phi_s,$$

$$M_d = m_d - 4G_S\phi_d + 2K\phi_u\phi_s,$$

$$M_s = m_s - 4G_S\phi_s + 2K\phi_u\phi_d$$

M. Buballa, Phys. Rept. 407, 205 (2005)

K. J. Sun et al., arXiv:2006.08929(2020)

4. Partonic interaction and equation of state

$$\mathcal{Z} = \text{Tr} e^{-\frac{1}{T}(\hat{H} - \mu\hat{N})} = \int D\psi D\bar{\psi} e^{\int_0^\beta \int \mathcal{L} d\tau d^3x}$$

$$\Omega = -\frac{T}{V} \ln \mathcal{Z} = \Omega_u + \Omega_d + \Omega_s + 2G_S(\phi_u^2 + \phi_d^2 + \phi_s^2) - 4K\phi_u\phi_d\phi_s - g_V(\rho_u + \rho_d + \rho_s)^2,$$

$$M_u = m_u - 4G_S\phi_u + 2K\phi_d\phi_s,$$

$$M_d = m_d - 4G_S\phi_d + 2K\phi_u\phi_s,$$

$$M_s = m_s - 4G_S\phi_s + 2K\phi_u\phi_d,$$

$$\mu_u^* = \mu_u - 2g_V(\rho_u + \rho_d + \rho_s),$$

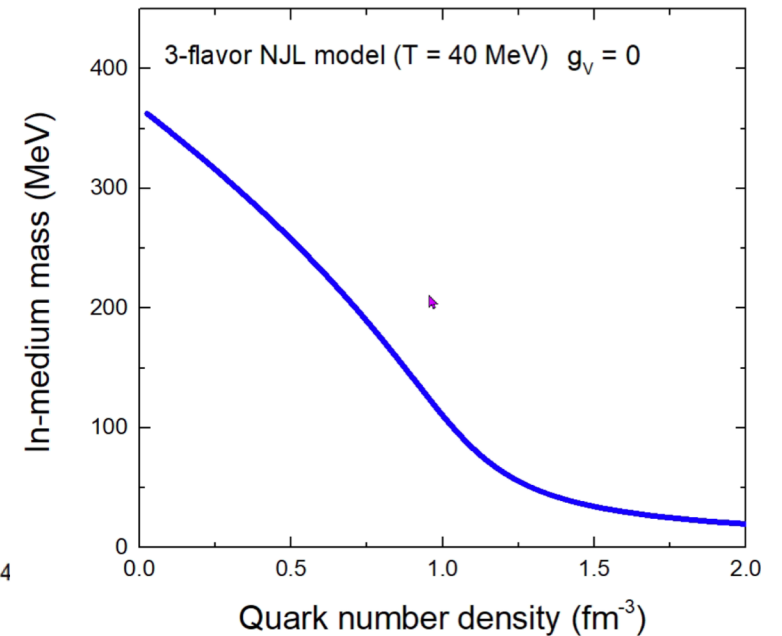
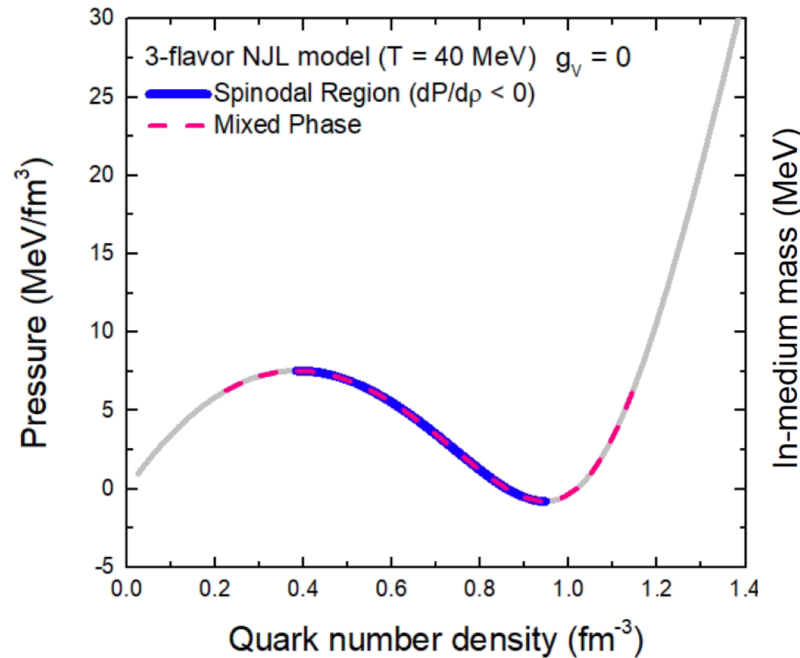
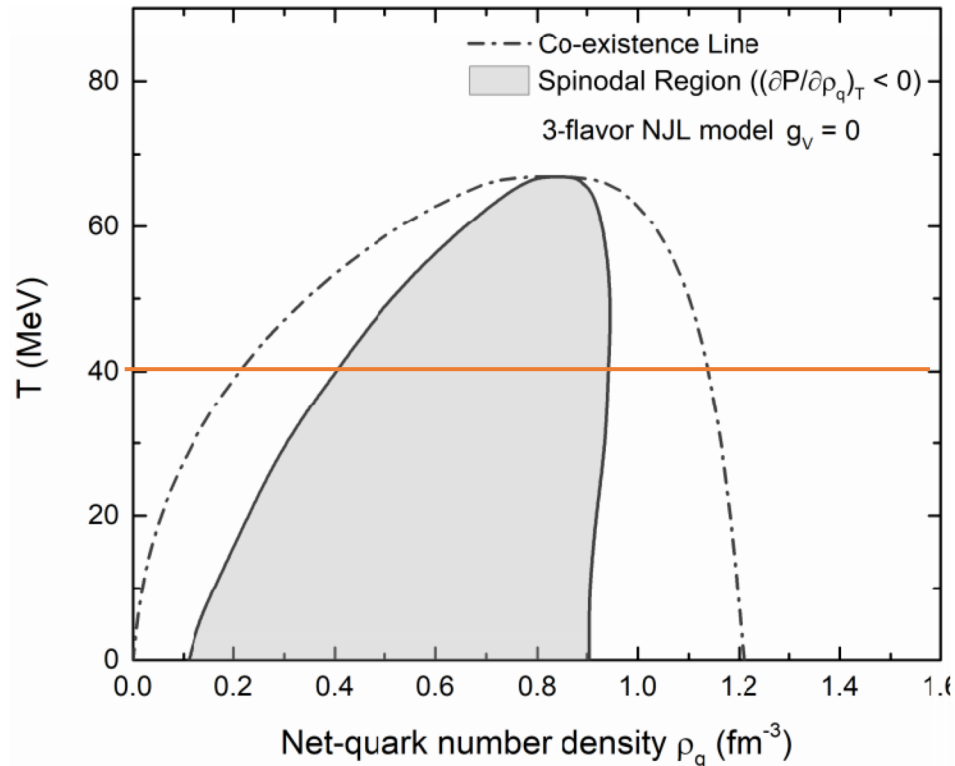
$$\mu_d^* = \mu_d - 2g_V(\rho_u + \rho_d + \rho_s),$$

$$\mu_s^* = \mu_s - 2g_V(\rho_u + \rho_d + \rho_s),$$

$$\frac{\delta\Omega}{\delta M_f} = \frac{\delta\Omega}{\delta\mu_f^*} = 0$$

$$\phi_f = 2N_c \int \frac{u^- p}{(2\pi)^3} \frac{M_f}{E_f} (n_{f+} + n_{f-} - 1),$$

$$\rho_f = 2N_c \int \frac{d^3p}{(2\pi)^3} (n_{f+} - n_{f-}),$$



4. Partonic evolution

Mean field + partonic scattering

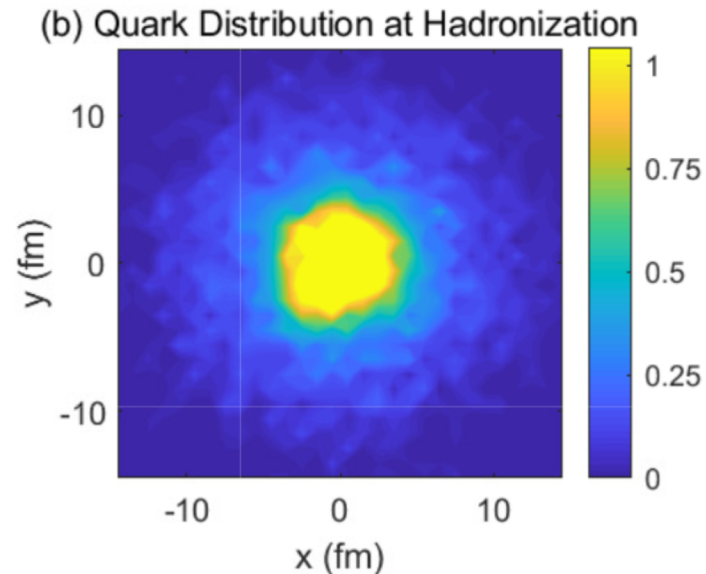
$$\begin{aligned} \frac{\partial f_{\pm}}{\partial t} + \mathbf{v} \cdot \nabla_r f_{\pm} + \left(-\frac{M}{E^*} \nabla_r M \pm \mathbf{E} \pm \mathbf{v} \times \mathbf{B} \right) \cdot \nabla_p f_{\pm} \\ = \left(\frac{\partial f_{\pm}}{\partial t} \right)_{\text{coll}} \end{aligned} \quad (16)$$

$$\mathbf{E} = -\frac{\partial \mathbf{A}}{\partial t} + \nabla_r \tilde{A}_0 \quad \mathbf{B} = \nabla_r \times \mathbf{A}$$

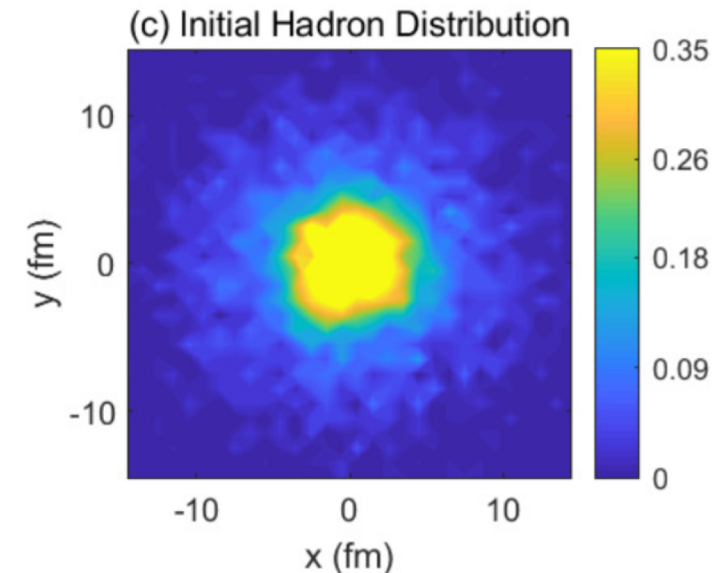
F. Li and C. M. Ko, Phys. Rev. C95, 055203(2017)

Hadronization through quark coalescence:

Z. Lin et al., Phys. Rev. C72, 064901(2005)



Quark coalescence



4. Enhancement of tp/d^2 and first-order phase transition

(32)

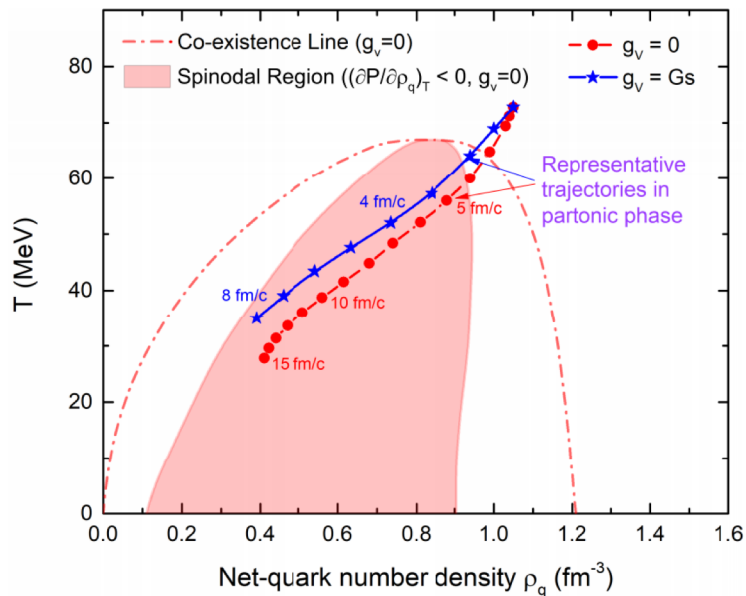
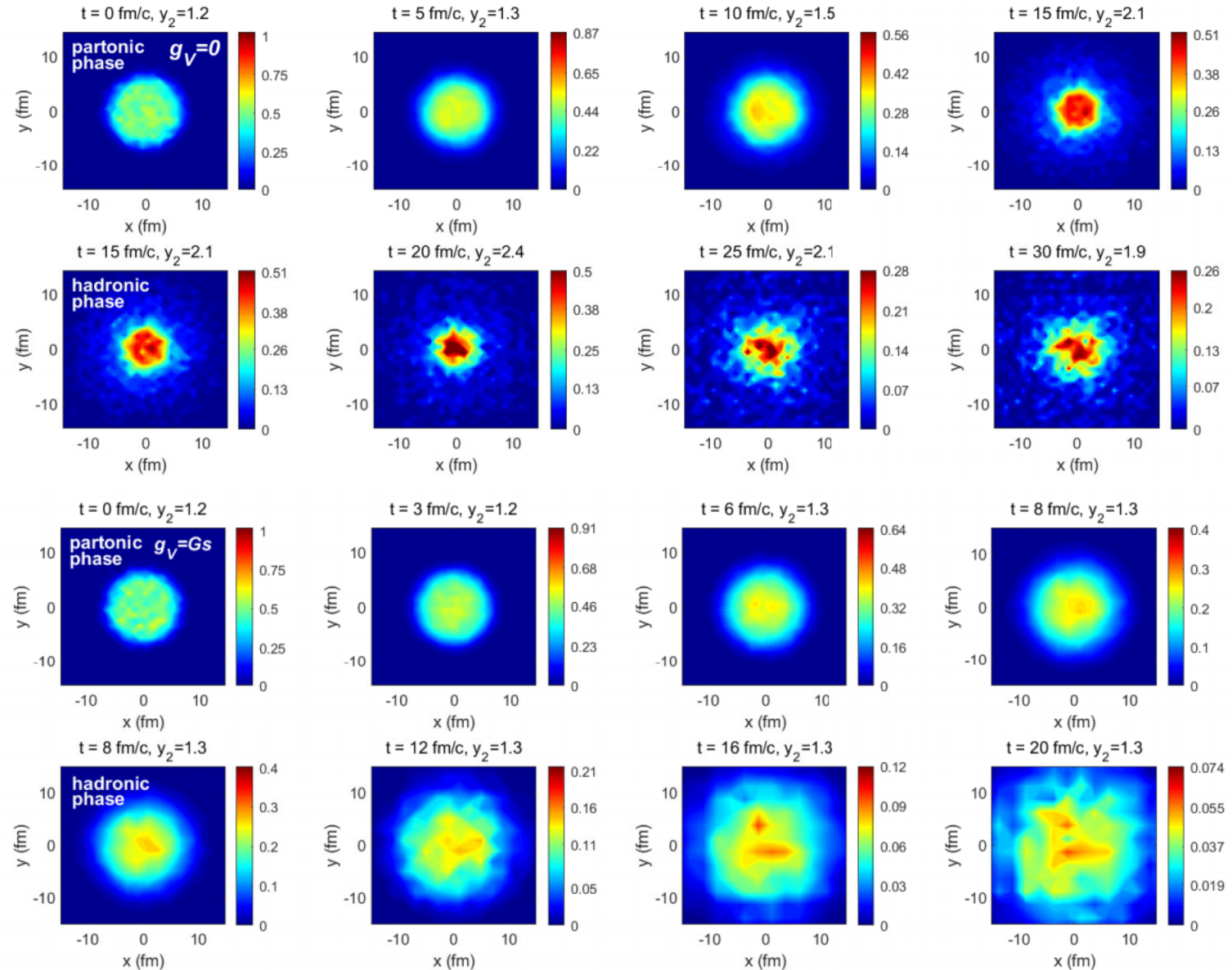
K. J. Sun et al., arXiv:2006.08929(2020)

Initialization:

$$\rho(r) = \frac{\rho_0}{1 + \exp((r - R)/a)}$$

$$R = 6 \text{ fm} \quad a = 0.6 \text{ fm} \quad \rho_0 = 1.5 \text{ fm}^{-3}$$

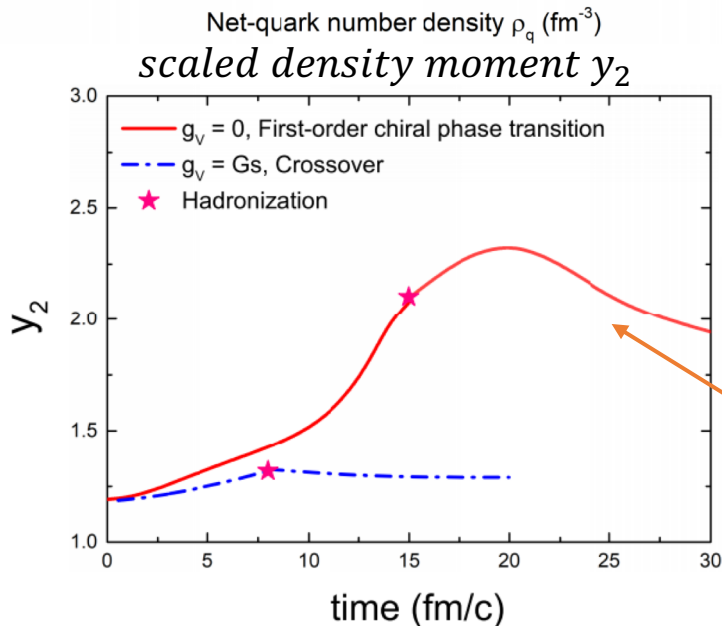
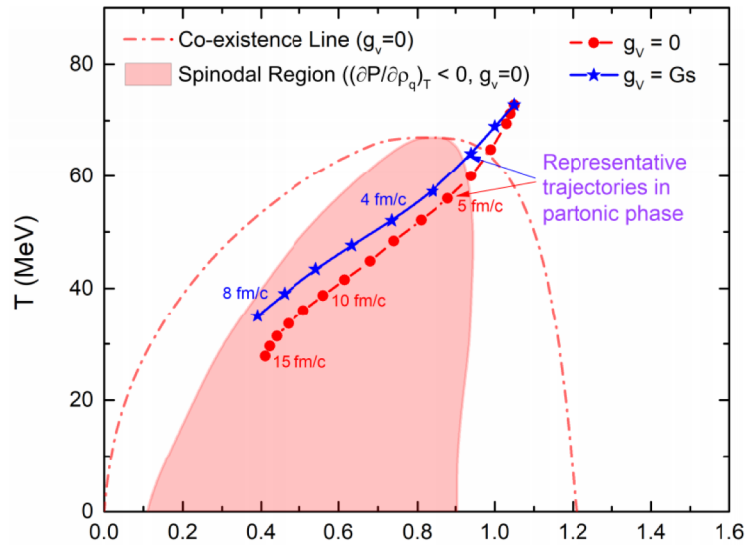
$$T = 70 \text{ MeV}$$



4. Enhancement of tp/d^2 and first-order phase transition

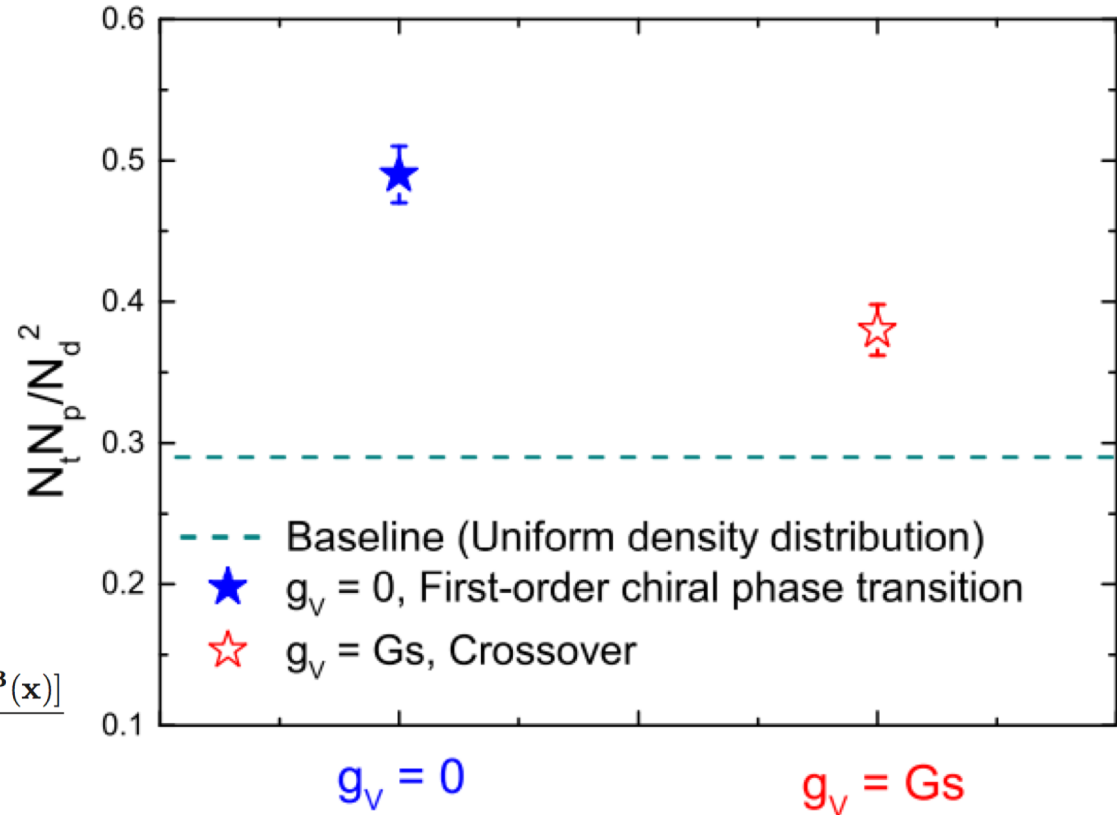
(33)

K. J. Sun et al., arXiv:2006.08929(2020)



$$y_2 = \frac{[\int d\mathbf{x}\rho(\mathbf{x})][\int d\mathbf{x}\rho^3(\mathbf{x})]}{[\int d\mathbf{x}\rho^2(\mathbf{x})]^2}$$

$$\approx 1 + \Delta\rho_n$$



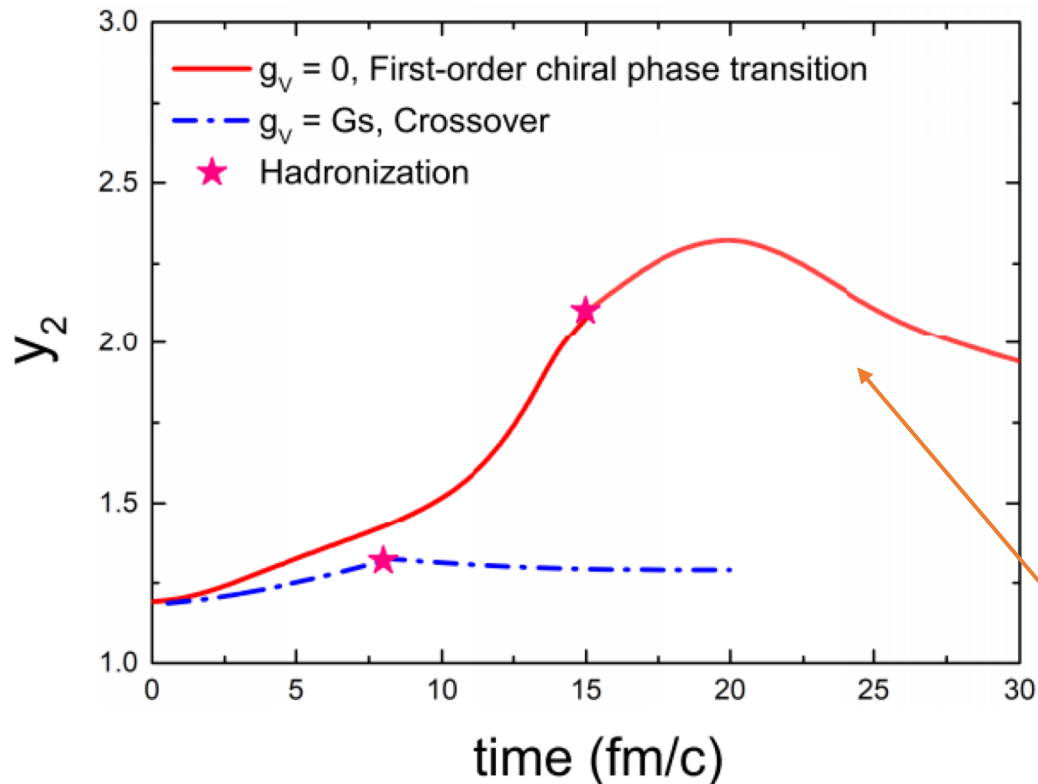
Further increasing g_v , this ratio remains unchanged

Large density inhomogeneity survives to kinetic freezeout

4. Off-equilibrium effects

(34)

K. J. Sun et al., arXiv:2006.08929(2020)



Density moment:

$$\overline{\rho^N} = \frac{\int d\mathbf{x} \rho^{(N+1)}(\mathbf{x})}{\int d\mathbf{x} \rho(\mathbf{x})}$$

$$y_2 = \frac{[\int d\mathbf{x} \rho(\mathbf{x})][\int d\mathbf{x} \rho^3(\mathbf{x})]}{[\int d\mathbf{x} \rho^2(\mathbf{x})]^2}$$

If the expansion is self-similar or scale invariant

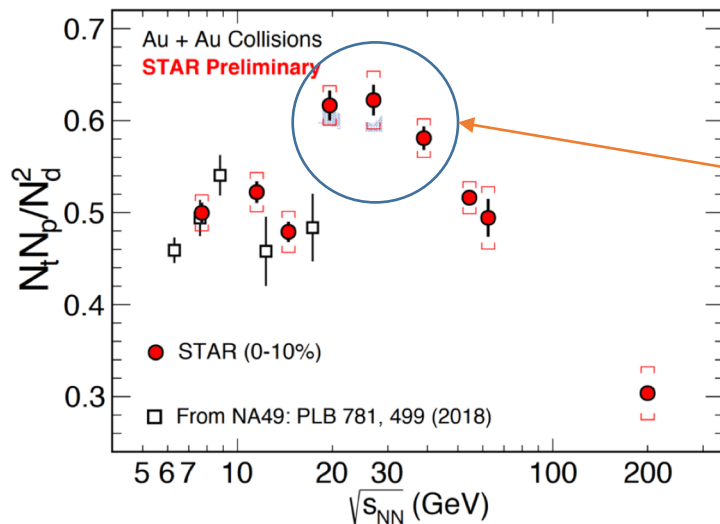
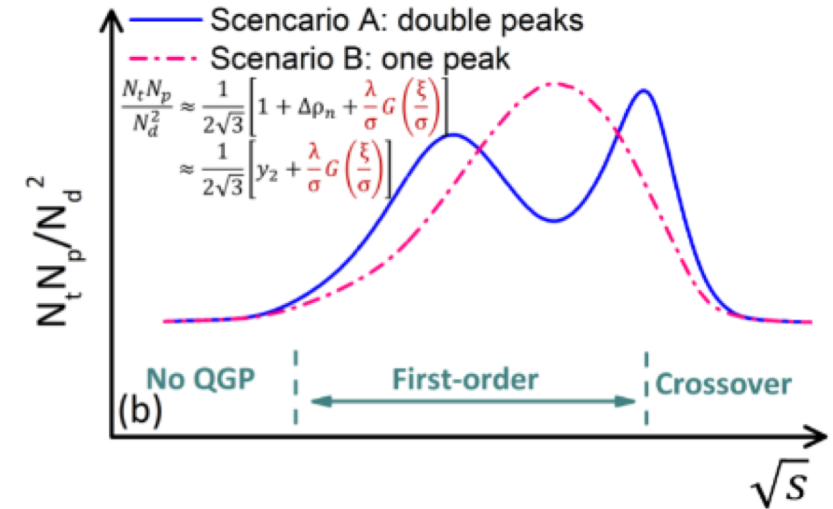
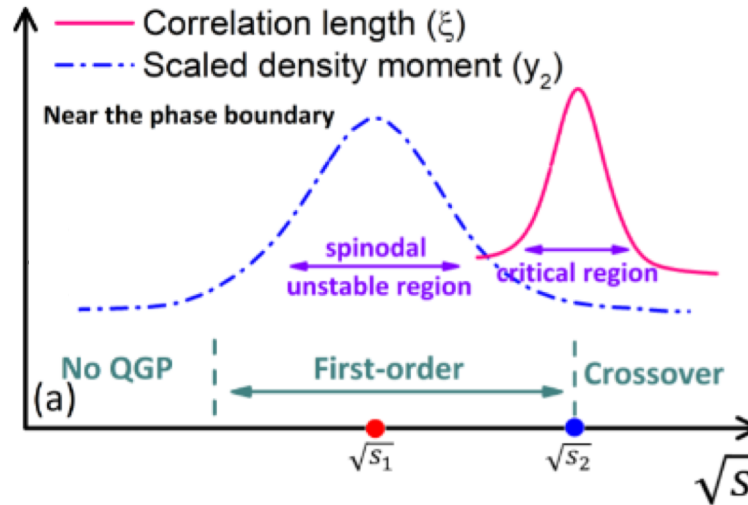
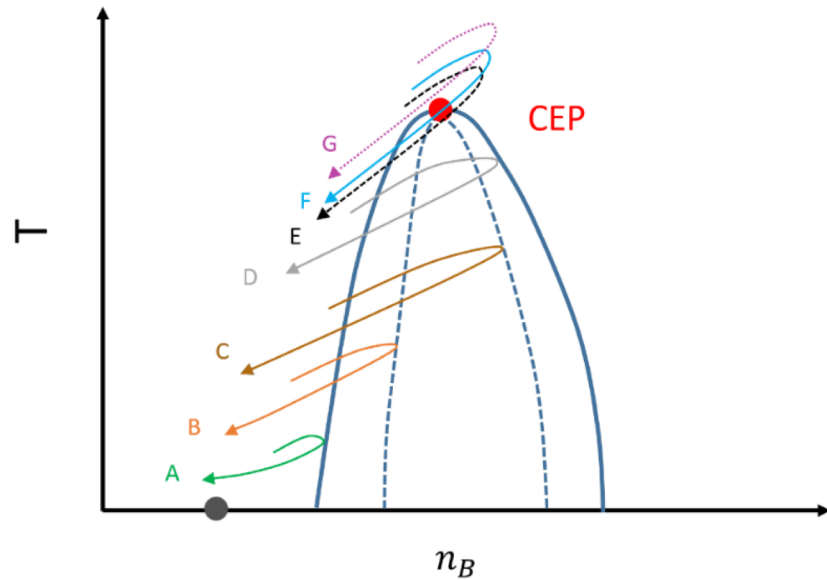
$$\rho(\lambda(t)x, t) = \alpha(t)\rho(x, t_h)$$

then $y_2(t) = y_2(t_h)$, i.e., remains a constant

Large density inhomogeneity survives to kinetic freezeout
Similarly, we expect such 'memory effect' also allows the long-range correlation to survive.

4. Collision energy dependence of tp/d^2

(35)



Signal from critical point?

Realistic dynamical modeling of the non-smooth quark-hadron phase transition within transport or hydro approaches is indispensable!

K. J. Sun et al., Phys. Lett. B 774, 103 (2017)

K. J. Sun et al., Phys. Lett. B 781, 499 (2018)

K. J. Sun et al., arXiv: 2006.08929(2020)

K. J. Sun, C. M. Ko, and F. Li, arXiv:2008.02325(2020)

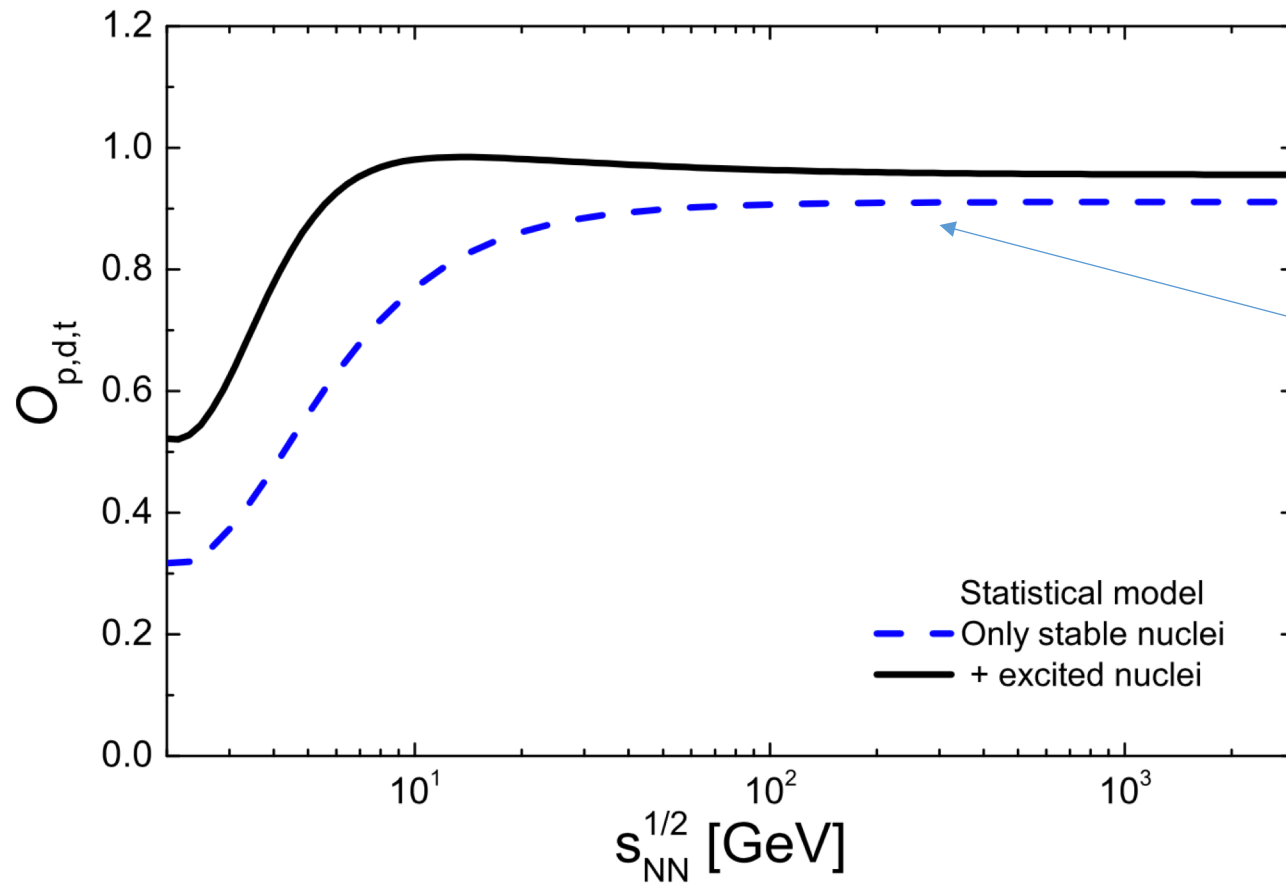
$$\frac{N_t N_p}{N_d^2} \approx \frac{1}{2\sqrt{3}} \left[1 + \Delta\rho_n + \frac{\lambda}{\sigma} G\left(\frac{\xi}{\sigma}\right) \right]$$

1. The long-range correlation near the QCD critical point leads to **enhancement** of light nuclei production and their yield ratios.
2. This novel phenomena of criticality opens up new possibilities to probe the QCD critical point with light nuclei production in relativistic heavy-ion collisions.
3. The observed **non-monotonic** behavior of tp/d^2 is likely due to the non-smooth phase transitions from QGP to hadronic matter.
4. To better understand the experimental results and locate the phase boundary in QCD phase diagram, we need better understanding of light nuclei production and better modeling of quark-hadron phase transition within transport or hydro approaches.

Thank you very much!

Backup

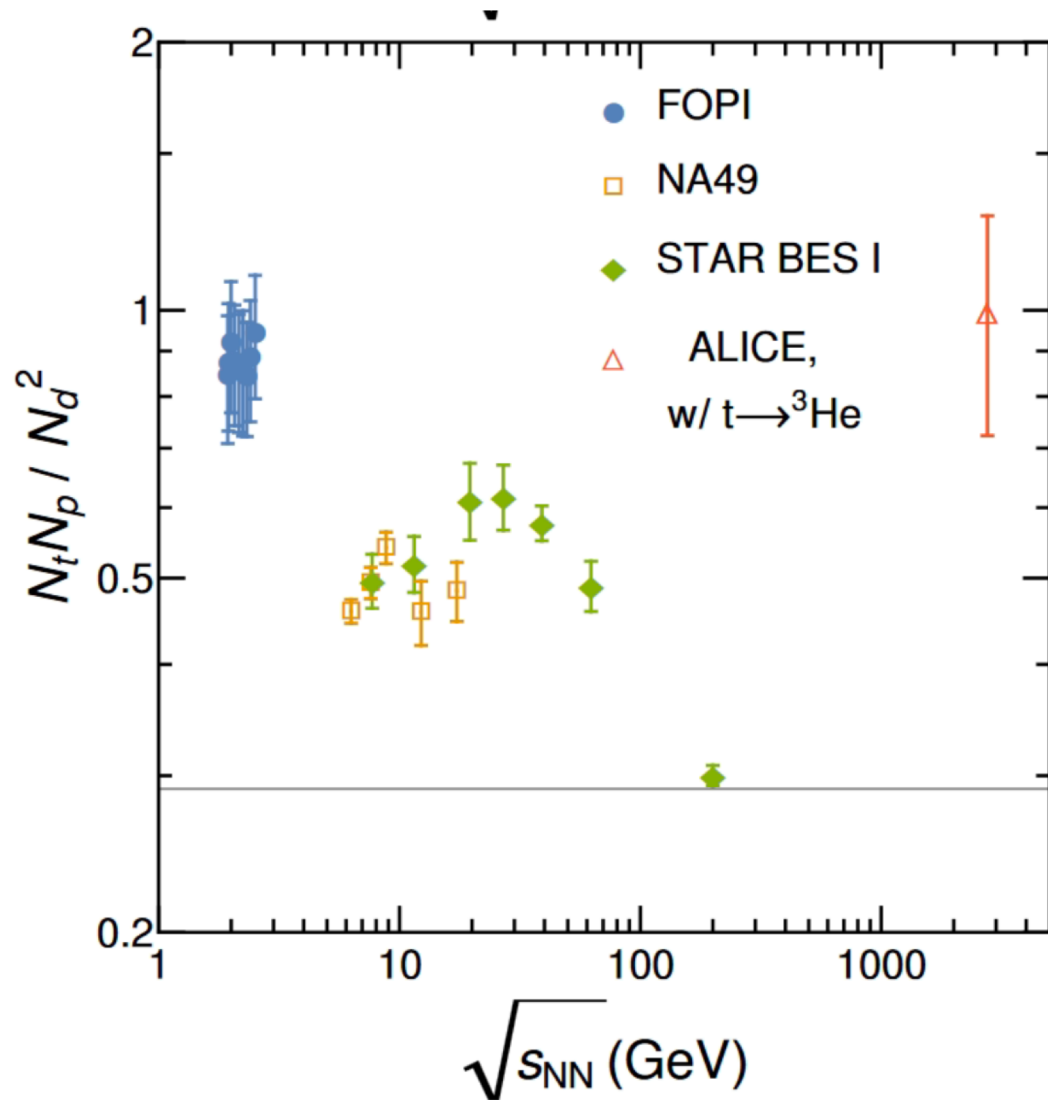
Thermal model



$$\frac{N_t N_p}{N_d^2} \approx \frac{1}{2\sqrt{3}} (1 + Res \rightarrow p)$$

Nucleons from decay of N and Delta resonances do not contribute to the deuteron and triton

Backup



1. Kinematics are different.
2. Production mechanisms at $\sqrt{s} \sim 2$ GeV might be different from that at RHIC and LHC energies.
3. Discrepancy between top RHIC energy and LHC energy needs to be understood.

Fig. from [E. Shuryak and J. M. Torres-Rincon, arXiv:2005.14216(2020)]